chemosensors

Review

Electrochemical Sensor for Food Monitoring Using Metal-Organic Framework Materials

Batoul Hosseinzadeh [1] and Maria Luz Rodriguez-Mendez [2,3,*]

[1] Department of Polymer Engineering and Color Technology, Amirkabir University of Technology, Tehran 1591634311, Iran; batoul.hosseinzadeh@outlook.com
[2] Group UVASENS, Escuela de Ingenierías Industriales, Universidad de Valladolid, Paseo del Cauce, 59, 47011 Valladolid, Spain
[3] BioecoUVA Research Institute, Universidad de Valladolid, 47011 Valladolid, Spain
* Correspondence: mluz@eii.uva.es

Abstract: Feeding the world's increasing inhabitants requires considerable quantities of food, whose quality is essential to personal and economic health. Food quality parameters are mandatory to control throughout the fresh produce supply chain to meet consumer requests. Until now, different analytical techniques have been employed in food safety control. However, most of these are laboratory needed, expensive, and time-consuming. To address these obstacles, many researchers have concentrated on developing electrochemical sensors (ECSs) as a powerful method with great sensitivity and reliability for food evaluation. Metal-organic frameworks (MOFs) with surprisingly porous morphology provide uniform yet tunable features, a high specific surface, and established practical applications in various fields. MOF-based ECSs present novel routes for the fast and effective detection of food contaminants or nutrients. In this current review, we concentrate on the MOF-based ECSs for food evaluation by first overviewing the library of available MOF sensors from pristine to MOF-bio composites and then exploiting recent application fields, with an emphasis on how this novel material unlocks new opportunities to monitor food nutrients or hazards.

Keywords: electrochemical sensors; metal-organic framework; food analysis

Citation: Hosseinzadeh, B.; Rodriguez-Mendez, M.L. Electrochemical Sensor for Food Monitoring Using Metal-Organic Framework Materials. *Chemosensors* **2023**, *11*, 357. https://doi.org/10.3390/chemosensors11070357

Academic Editor: Núria Serrano

Received: 15 May 2023
Revised: 20 June 2023
Accepted: 21 June 2023
Published: 25 June 2023

1. Introduction

Food quality is a complicated outline that is regularly measured employing objective indicators attributed to the nutritional, microbiological, or physicochemical properties of the food. Quality is a critical parameter in modern food industries since the high quality of the product is fundamental for success in the present competitive business environment. Thus, food quality and safety have been highly trendy for the last 10 years—in popular interest, in the food industry, and, in research and the implementation of new techniques to assess the quality and safety of food—which is of considerable significance to today's industries. To achieve this aim, it is of great importance to develop a rapid, sensitive, and powerful technique for food monitoring to prohibit, control, and lighten the effects of potential outbreaks. However, quality control and monitoring the contaminants in food samples have been faced with significant difficulties due to complicated matrices and potential interference [1]. Although conventional analytical methods such as chromatographic and spectroscopic techniques would meet most of the necessities in this field, complex sample pre-processing, laborious instruments, skilled laboratory personnel, and time-consuming procedures restricted their practical applications [2–6]. In this view, electrochemical (EC) sensing methods, with the benefits of being sensitive, rapid, low sample consumption, and uncomplicated operation, have been introduced as a reliable substitute for traditional methods and have attracted significant attention in this field [7–9].

In electrochemical sensors (ECS), the critical sensing features, including high efficiency, sensitivity, selectivity, and stability, are settled mainly by the design of sensing

elements. The applicability of this detection technique has been improved with the recent advancement of new functional materials, including carbon-based materials, conjugated polymers, metallic oxide nanomaterials, and metal-organic frameworks (MOFs) [10,11]. These materials are anticipated to play dominant roles in overcoming severe difficulties and attaining progress for the ECS in food evaluation. Recently, nanotechnologists have announced various kinds of revolutionary materials for particular applications. Among them, MOFs have emerged as a state-of-the-art material for analytical sensing.

Metal-organic frameworks (MOFs) are a class of porous crystalline materials that are fabricated from metal-based nodes and organic bridging ligands through coordination binding, present ultrahigh surface areas, tunable porosity, controllable and captivating morphologies, and adaptable surface characteristics [12]. As a result of their tunable physical and chemical features, MOFs have been frequently utilized in various fields, such as gas storage, catalysis, energy storage, contaminant removal, and drug delivery [13–16]. They have also displayed great potential as promising EC sensing platforms owing to the following aspects: (1) MOFs have unsaturated metal coordination sites, periodic lattice morphology, and distinctive structural properties. These noticeable characteristics equip MOFs with excellent catalytic ability and make them valuable as practical coating substances for electrocatalytic electrodes applied in sensing systems. The main benefits of using MOFs as a sensing material to acquire better analytical performance arise from their distinctive and highly tunable physicochemical/structural features. At first, skim sensitivity seems to be attributed to the power of the analyte/MOF interaction, where stronger binding results in lower DL. The strength of the analyte-MOF binding can be obtained through pore size diversity, the hydrophilicity-hydrophilicity of the pores, specific functional groups, or functionalization with biomolecules that provide extra affinity between analytes and functional groups or open metal sites (OMS). For instance, in the case of nanosized MOFs, owing to their higher surface-to-volume ratio and shorter diffusion paths, they have better sensitivity and a quick response. Selectivity provided by MOF-based sensors is related to pore and aperture sizes; for example, size exclusion of larger molecules leads to enhanced selectivity. As the MOF porosity can be regulated via composition changes by optimizing node or linker sizes, geometries, linker attachments, and their directional orientation, which provides not only the pore and aperture size changes but also its hydrophilic-hydrophobic properties to raise the specific tendency towards the target molecules. The stability of MOFs arises from various parameters like the type, geometries, characteristics of the linkers and of the metal centers, the strength of the coordination bonds, and the MOF topology, as well as the particle sizes of the MOFs. Among them, the power of the M-linker binding has been demonstrated as the most dominant parameter of the MOFs stability, and more interestingly, it can be strong enough not to break upon specific sensing conditions. As a result of this chemical and physical stability, the repeatability and reproducibility of MOF-based sensors has been improved. MOFs also offer various advantages that play a critical role in improving the reliability of sensors. For example, a stable and protective environment can be obtained through the integration of electroactive species or catalysts within porous structures. This prevents the degradation or leaching of sensing elements, resulting in their protection from externally inappropriate factors that can negatively influence repeatability. Additionally, precise immobilization of analytes or target molecules within the well-organized structure of MOFs leads to uniform interaction between the sensing elements and the target analytes, which results in consistent and reproducible responses. Further, the selective capture of specific molecules minimizes interference from other substances. This selectivity improves the reproducibility of measurements by reducing false-positive or false-negative readings, thereby enhancing the reliability of the sensor. MOFs can also be used as thin film coatings on electrode surfaces, providing a controlled environment for electrochemical reactions. These MOF films ensure uniform and well-defined electrode-analyte interactions, contributing to improved repeatability. Additionally, the films act as barriers to prevent interfering species from reaching the electrode surface, further enhancing the reproducibility of the sensor. Encouraged by these charming characteristics, a variety of pristine MOFs with exceptional electroactivities have been directly applied as electrocatalysts

to detect different small molecular substances, including H_2O_2, glucose, dopamine, heavy metals, and [17–20].

In previous literature, researchers have presented applications of MOFs in various areas of food safety and quality, like production, packaging, storage, and detection. Radhakrishnan, Chen, Zhang, and Cheng overviewed MOF-based materials from the point of view of synthesis, and applications in the detection of pollutants in food [21–23]. Su et al. presented advancement and challenges in MOFs utilization as chemical sensors [24]. However, until now, no comprehensive review concentrated on the MOF-based ECSs for food evaluation has been available. In the current review, we provide an overview of the different MOF-based materials used to design ECS for food analysis. The available utilization is summarized and discussed based on the target analyte detection. The most important types of MOF-based materials are also explored in ECS fabrication.

2. Application of MOF-Based Materials for Electrochemical Food Monitoring

Food analysis is essential for quality observation and safety approval. Recently, it has seen a drastic growth in novel analytical methods utilized in food quality confirmation. Along with this, there has been a parallel prosperity in the functional materials area to improve selectivity, sensitivity, and stability. Owing to their unique characteristics, MOFs present a niche in the material field, enabling them to become an essential and highly favorable part of the food industry. To date, MOF has demonstrated its capabilities in various aspects of the food industry, including contamination removal, food packaging, improvement of food preservation, and monitoring of food products. Many researchers have recently concentrated on applying MOFs in sensor development for food evaluation, such as fluorescence, EC, colorimetric, and surface-enhanced Raman scattering (SERS) sensors [25,26]. Among them, MOF-based ECSs have attracted immense attention because the superiority of MOFs relies on two essential parameters: high surface area and extraordinarily tunable structures. They also displayed outstanding anchoring capacity for chemical functionalization by different functional groups like $–NH_2$ and –COOH through in-situ or post-modification [27,28]. These characteristics make MOFs ideal candidates as a supporting platform for co-immobilizing catalysts and enzymes via interactions like hydrogen bonding, π–π stacking, and electrostatic interaction between MOF and biological ligands [29,30]. Improvement of key physio-chemical characteristics of MOFs can also be performed through combination or scaffolding with a variety of functional substances like metal oxide nanoparticles, metallic nanoparticles, quantum dots, polyoxometalates, and carbonaceous materials (carbon nanotubes, graphene (Gr), etc. [31,32]. These classes of MOF-based composites present exceptional physiochemical features that cannot be obtained with pristine MOFs. In recent years, a variety of MOF composites have been introduced with excellent stability in severe conditions (highly acidic or base), improved catalytic activity, and increased signal transduction in sensing investigations. In the context of evaluating food-based analytes using electrochemistry, MOF-based modifiers can play different roles, such as improving electrochemical performance by increasing the effective surface area of the electrode, resulting in more active sites for analyte adsorption, and facilitating electron transfer processes. Furthermore, analyte preconcentration can be carried out by MOFs by selectively adsorbing specific analytes from complex food matrices onto their porous structures. This preconcentration step assists in overcoming the challenges related to trace analyte contents, interference, and the complexity of sample environments. Therefore, MOF materials are favorable in sensor development, and in the following section, recent advancements in MOF-based ECSs in sensor development for food analysis and related studies are reviewed.

2.1. Heavy Metal Ions

Heavy metals are elements spread in trace amounts in nature, a number of which, in low quantities, perform an essential role in human bodies; even so, they could give rise to perniciousness in higher concentrations [33]. Moreover, Pb and Cd are very poisonous

pollutants that could have critical unfavorable health impacts, and food and water are the main sources of these toxic metals introduced to living organs. Therefore, to protect users, the quantity of heavy metals should be repeatedly and quickly determined at different steps of the food chain [34].

MOFs have been employed to monitor heavy metal contamination in food samples at trace concentrations. Incorporating MOFs with reliable facilities, such as EC techniques, enhances the sensitivity of recognition and enables researchers to develop a novel direction for improving the analytical performance of detection systems. In this context, Wang et al. fabricated a new ECS using graphene aerogel (GA) and UiO-66-NH_2 crystals with alternating octahedral and tetrahedral cages to fabricate a hybrid for simultaneous detection of various heavy metal ions in the aqueous medium [35]. The hybrid material of GA/MOF was prepared by the in-situ formation of UiO-66-NH_2 MOF on the GA substrate as a backbone frame, raising electrical conductivity. Investigation of the obtained material morphology using SEM and TEM revealed a wrinkled and interconnected network with opened macropores for Gas in which octahedral cubic UiO-66-NH_2 crystals accumulated randomly within the GA matrix. The XRD patterns of UiO-66-NH_2 and GA displayed sharp diffraction peaks, confirming high crystallinity, which showed the GAs did not destroy the structure of MOF. the According to obtained findings, the GA–UiO-66- NH_2/GCE could successfully detect the Cu^{2+}, Hg^{2+}, Pb^{2+}, and Cd^{2+} in with excellent sensitivity even in the presence of various interferent metal ions with high concentrations. The DLs were achieved as 0.9 nM, 1 nM, 8 nM, and 9 nM for Hg^{2+}, Pb^{2+}, Cu^{2+}, and Cd^{2+}, respectively. This approach also provided acceptable results for sensing the ions in vegetable and soil solutions with high accuracy.

In another study, Hung and colleagues investigated the potential of a new ECS for the detection of Hg^{2+} ions in canned tuna fish [36]. The ultra sensitivity, improved electron transfer, and stability were obtained through a combination of polyvinyl pyrrolidone (PVP) and the Cu-MOF frame. The porous cubic geometry gave a higher number of edge defects and free –NH and -OH functional groups, which could display high affinity toward Hg^{2+}, resulting in its reduction on the surface of the electrode. The DL of Hg^{2+} was obtained to be 0.0633 nM in a linearity range from 0.1 to 50 nM. A voltammetric sensor for cadmium ions (Cd^{2+}) detection in meat samples, based on amine-functionalized Zr(IV)-MOF (UiO-66-NH_2) and MWCNT composite fabricated through a one-pot hydrothermal reaction was reported by Zou et al. [37]. The prepared sensor displayed outstanding EC activity, with an excellent linear range from 0.5 to 170 μg/L and a DL of 0.2 μg/L for Cd^{2+} detection with a recovery of 95.1–107.5%. The plentiful amino groups in UiO-66-NH_2 simplified the preconcentration of Cd^{2+} on the electrode interface. Exploiting the high affinity of amino and carboxyl functional groups toward metal ions, Lin and colleagues also presented an EC constructed of a NH_2-MIL-53(Al)/polypyrrole (PPy) hybrid structure coated on a gold electrode [38]. The nanocomposite-modified electrode displayed sensing activity toward Cu^{2+} and Pb^{2+} with a DL of 0.244 μg L^{-1} and 0.315 μg L^{-1}, respectively, with great selectivity in the presence of other popular interferences. The adsorption volume of the chelating groups reduced in the order of Cu ≫ Pb ≫ Cd ≫ Zn ≫ Ni, Hg.

Cui et al. fabricated 3D origami ECS for sensitive and selective determination of Pb^{2+} in different water, fruit juice, and real soil samples using a novel designed DNA functionalized iron-porphyrinic MOF (Fe-)$_n$-MOF [39]. Immobilization of porphyrin groups within the tight morphology of MOF platforms not only help porphyrin be available on substrates but also inhibits the dimerization of reaction centers, which is destructive for its catalytic performance. The stable (Fe-P)$_n$-MOF could provide multiple signal types to obtain high sensitivity; simultaneously, the Gr, which was joined to the structure through the Au particles (AuNPs), gave excellent selectivity for this applied technique.

In novel research, Papaefstathiou et al. prepared a new 3D-printed lab-in-a-syringe tool using a 2D Ca-MOF, which offers sorption affinity and exchanged characteristics to multiple metal ions [40]. They demonstrated that the Ca-MOF is a highly productive Hg^{2+} sorbent with fast adsorption kinetics. Their work was the first combination of MOF

electrode modifiers via a one-step procedure employing a dual extruder 3D printer. The fabricated device displayed improved electroanalytical properties, which were employed for Hg^{2+} quantification in fish oil and bottled water samples.

An ultra-sensitive EC DNA sensor for the determination of Hg^{2+} in dairy industry outputs was fabricated by Zou et al. [41]. Cu-MOFs were employed as DNA carriers to design signal probes and enzyme-free catalytic amplifiers. Additionally, GO@AuNPs composite was employed to fabricate a conductive interface. Exploiting the thymine-Hg^{2+}-thymine (T-Hg^{2+}-T) complex formation, a good anti-jamming capability to detect Hg^{2+} in the complicated environment would be obtained. This method presented an ultrasensitive scrutiny of Hg^{2+} within the concentration range from 0.10 aM to 100 nM with a DL of 0.001 aM. Similarly, they employed another Cu-MOF for on-site analysis of quality deterioration in dairy products contaminated with Hg^{2+} [42]. The obtained DL of 4.8 fM was reported for this strategy. Considering the severe importance of Pb^{2+} detection in ultralow quantities and using a similar strategy in exploiting MOF as a peroxidase-mimicking catalyst for signal amplification, Shi and coworkers synthesized the incorporated porphyrin HKUST-1(Cu) [43]. Utilizing the specific identification of DNAzyme for Pb^{2+}, the suggested procedure demonstrated satisfactory anti-jamming capability for Pb^{2+} sensing in the presence of interferences with the capability to sense Pb^{2+} contaminants in leaf vegetables.

2.2. Food Additives

In recent years, food additives have become a severe threat to community health and food protection [44]. Food adulteration is explained as the insertion or extraction of any materials to/from food that impact the natural condition and constitution of the food substance. Sudan dyes have been recognized in flavoring powders, pepper sauces, piquant soups, colorful snacks, and even soda. Such illegal artificial dyes, including Sunset Yellow (SY), Sudan Red, and Ponceau 4 R, are non-expensive and accessible as colorants to intensify the natural color or improve the appearance, taste, and composition of products [45]. However, most of them have an aromatic ring in their chemical structure that is harmful to human health when extended. Contamination of natural milk with synthetic materials is also an important issue in different communities. For instance, melamine is a synthetic substance with a high quantity of nitrogen, which is frequently employed in melamine resin preparation. Recently, it has been illegally poured in milk to incorrectly display a higher amount of protein, which is typically determined based on nitrogen content with the Kjeldahl procedure, resulting in dangerous sickness and health risks [46]. Therefore, monitoring illegal additive chemicals at trace concentrations would be beneficial.

Malachite green is beneficial in cases of parasite and microbial contagion in fish. However, as a chemical substance, malachite green would occupy their organs for a long time, resulting in ramifications. Recently, malachite green has been illegitimately employed in the aquaculture industry. To sensitively detect malachite green, Zhou and coworkers developed a new ECS utilizing Ag/Cu-MOFs prepared in a single-step solvothermal procedure [47]. MOF identification was carried out by XPS measurements. Besides photoelectron peaks related to C, O, and Cu, doublet peaks attributed to Ag 3d3/2 and Ag 3d5/2 were observed. The Ag/Cu proportion was calculated to be 7.65%, which was in agreement with the EDS experiment. The higher values of binding energy compared to common chemical states of Ag are attributed to the four electronegative oxygen atoms of carboxylic ligands, which lead to larger inner electron binding energies. This result confirmed that the mixed-node MOFs (Ag/Cu-MOFs) were successfully prepared by the one-step synthesis. According to CV studies, malachite green displayed well-defined oxidation peaks around 0.57 V without a cathodic peak on the reverse sweep, indicating an irreversible process. Investigation of the relation between scan rate and the oxidation peak potential revealed a peak shift to a less positive value with the increase in scan rate, with Na estimated to be 2. This is explained as follows: The electrochemical oxidation of malachite green occurs with the ejection of an integral unit of the central carbon connected to a phenyl group, followed by the intramolecular coupling of two phenyl fragments. This process is an

electrochemically irreversible, two-electron transfer process. In comparison with the bare electrode, the modified one efficaciously resulted in more sensitive detection with a low DL of 2.2 nM in a linearity range of 10–140 nM and an acceptable anti-interference potential. In another study, a highly sensitive, conductive, and selective sensor has been introduced by Shabani-Nooshabadi and colleagues for simultaneous measurement of tartrazine, patent blue V, acid violet 7, and ponceau 4RA in food products like jellies, condiments, soft drinks, and candies [48]. A modified carbon paste electrode was prepared using copper-based MOF (Cu-BTC MOF) and 1-ethyl-3-methylimidazolium chloride as an ionic liquid (IL) to improve the surface area and conductivity and, consequently, electron transfer rate enhancement. The excellent analytical performance of the suggested system was approved for patent blue V by providing a low DL of 0.07 μM, a broad linearity range between 0.08 and 900 μM and reasonable recovery.

Exploiting MOF for the determination of another azo dye of SY was carried out by Ji and coworkers [49]. Besides the high electrocatalytic activity of Fe-BTC, owing to its surface area of 637.8 m^2/g, the accumulation potential of SY is enhanced dramatically, which helps it show great EC performance toward detecting SY in various complex drink matrices. Another sensitive sensor for SY was fabricated by Qi and coworkers using cetyltrimethylammonium bromide (CTAB) functionalized with Gr and Cu/Zr-MOF [50]. This novel CTAB-Gr-Cu/Zr-MOF hybrid structure was fabricated via electrostatic interaction between CTAB-Gr and Cu/Zr-MOF and employed for detecting SY in soft drinks. In comparison with the bare electrode, the newly modified one surprisingly enhanced the EC current by 6.53-fold and provided DL in nM order.

Nitrite is a popular additive to meat in the food industry as a coloring and disinfectant substance. However, the consumption of nitrite at a higher than appropriate value leads to an undesirable effect on human health. In the past few years, MOFs have also been employed to construct EC platforms for nitrite sensing. For example, Adarakatti and coworkers presented an EC system for nitrite determination via an MWCNT-decorated Co-based MOF-modified electrode [51]. The synergetic effect between the two components, resulting in feasible nitrite oxidation on the electrode surface, and the practical applicability of the designed sensor for analyzing the packed beverage sample. In another work, a gold-platinum alloy nanocomposite was electrochemically deposited on a copper-based MOF by Gu et al. [52]. The porosity of the Cu-MOF structure inhibited the agglomeration of Au@Pt NPS, assisting the nanoparticle in showing better activity. In addition, the specific morphology of MOF to adsorb higher concentrations of nitrite, in combination with the great catalytic performance of alloy particles, promised the sensor exceptional performance for nitrite detection in food samples of mustard and ham sausage.

An analysis platform with great potential to determine nitrite in milk, sausage, and pickled vegetables was also developed via encapsulated Au NPs and rGO inside the Cu-TDPAT (TDPAT = 2, 4, 6-tris(3, 5-dicarboxylphenylamino)–1, 3, 5-triazine) [53]. The surface morphologies of composites were studied by SEM, which illustrated that AuNPs were uniformly deposited on the structure. The crystallinity of the material was also investigated by XRD, and the obtained findings displayed a peak at $2\theta = 10.6^\circ$ related to GO and characteristic diffraction patterns of MOF, confirming the successful synthesis of the composite. The oxidation responses of nitrite at different modified electrodes were evaluated using the CV method. According to findings, the nitrite oxidation peak potential was 0.903 and 0.77 V at the bare GCE, Au/ERGO/Cu-TDPAT/GCE, respectively, which means easier nitrite oxidation on the modified electrode as a result of the electrocatalytic activity of the proposed composite. Additionally, the oxidation response of nitrite on Au/ERGO/GCE had a small anodic peak, while on Au/ERGO/Cu-TDPAT/GCE, nitrite showed the largest peak, approximately 5.4 times higher than those on the bare electrode. These observations demonstrated the unexceptionable role of MOF in loading ERGO and AuNPs to enhance the catalytic efficiency of electrodes. The results also displayed a linear relation between the oxidation peak current and the square root of the scan rate, indicating a diffusion-controlled oxidation process of nitrite.

In a different configuration, Asadpour-Zeynali and his colleague fabricated the Core-shell ZIF-8@ZIF-67/Au NPs as a novel electrode modifier to sense nitrite [54]. As a usual subclass of MOF, imidazole zeolites (ZIFs) are full of carbon, nitrogen, and transition metals with extraordinary thermal and chemical stability in addition to their easy, costless preparation. In fact, zeolite imidazolate frameworks are a combination of the characteristics of both zeolites and MOFs. To study the electrochemical behavior of nitrite on the modified electrode, the voltammogram cycle was recorded. By adding nitrite to the bare electrode, a peak at 1.1 volts was observed. On the modified electrode with ZIF-8@ZIF-67, the nitrite oxidation peak was at 0.99 V, and on the modified electrode with ZIF-8@ZIF-67/Au NPs, the irreversible oxidation peak at 0.77 V appeared. This oxidation current in the electrode modified with ZIF-8@ZIF-67/Au NPs was also higher than other electrodes, which can be attributed to the synergetic effect of the ZIF-8@ZIF-67 to increase the surface area and the enhanced conductivity owing to the presence of gold metal nanoparticles. All these properties gave an excellent catalytic impact for nitrite oxidation and consequently reliable nitrite measurement in real samples of sausages, deli meat, and drinking water in a short time. Dong et al. also developed an ECS for nitrite detection in pickle juice samples using a Co-TCPP/ionic liquid/Cyt c bio-hybrid. In their work, Cyt c was immobilized onto Co-TCPP, followed by the ionic liquid integration. After keeping it for 14 days at 4 °C in an environment with a pH of 7.0, the fabricated sensor maintained 91% of its initial signal, confirming its great stability.

2.3. Foodborne Pathogens

The common foodborne pathogens are known as norovirus, Salmonella, Clostridium perfringens, Campylobacter, and Staphylococcus aureus, most of which are bacterial. Besides them, Clostridium botulinum, Listeria spp., Escherichia coli, and Vibrio spp. are also serious foodborne pathogens that make infections a requirement for hospitalization [55,56]. Thus, foodborne toxins pose an important and serious threat to world health. One valuable activity to overcome bacterial foodborne disease is improvement in pathogen detection prior to human infection. Since the environments in which these pathogens are present vary from food packaging instruments to restaurants and home kitchens, detection techniques for contagions must be low-cost, easy to use, and rapid while being stable, sensitive, and selective. Among the various available methods, EC sensing is uniquely suitable for point-of-contaminant detection [57]. In the field of mycotoxins sensing, most utilizations of these novel materials are based on their integration with specific target detection elements, including aptamers, antibodies, and molecularly imprinted polymers (MIP). For instance, He and his coworker presented an ultrasensitive EC aptasensor utilizing $CoSe_2$/Au nanorods, 3D-structured DNA-PtNi@Co-MOF, and nicking endonuclease to determine the zearalenone (ZEN) [58]. The Co-MOF is prepared to improve the aptasensor sensitivity, and the PtNi nanostructure is used for both immobilization DNA and thionine (Thi) via Pt-N or Pt-S connections to make a three-dimensional network and to provide synergetic catalytic influence with the Co-MOF towards signal tags such as Thi. The $CoSe_2$/Au is also employed to provide total activity of the nicking enzyme and DNA-PtNi@CoMOF networks in signal increase. In the presence of ZEN, the aptamer forms a complex with ZEN via a nicking enzyme, leading to DNA H1 production. Consequently, a significant Thi signal could be discerned because of the incubation of Thi-labeled DNA H2–PtNi@Co-MOF and DNA-PtNi@Co-MOF networks onto the aptasensor. In comparison with traditional hybridization chain reactions, the DNAPtNi@Co-MOF structure can couple with abundant signal tags (Thi), as well as present multiple signal boosters (PtNi@Co-MOF). Additionally, the aptasensor displayed an appreciative response to ZEN evaluation in maize samples, establishing the applicable capacity for mycotoxins detection.

In spite of the strong investigations into MOF-DNA linkage, the utilization of MOF-DNA links has been restricted because of the complicated modification process. Amongst various MOFs, Zr-based MOF (UiO-67) contains Zr-OH groups, originating from the missing-linker-prompted terminal hydroxyls and the innate bridging ones in Zr-O clusters [59,60]. The UiO-67 displays great affinity for phosphoric groups by making a complex

of Zr-O-P, which makes it pleasant to form a single-step connection between the UiO-67 and phosphate-terminal DNA probes. Wang et al. used the UiO-67/Gr composite for ultrasensitive detection of S. Typhimurium in milk samples [61]. Through this designed system, S. Typhimurium was successfully determined with a DL of 5 CFU/mL within a linearity range from 2×10^1 to 2×10^8 CFU/mL.

Jiang and colleagues introduced a novel impedimetric sensor based on a Mn-based MOF (Mn-MOF-74) for fast and sensitive detection of Listeria monocytogenes (L. m) [62]. At first, the capture antibodies (Ab1) were utilized to modify the surface of the magnetic substrate to prepare immunomagnetic beads (MBs@Ab1) capable of precisely taking apart L. m cells from the milk matrices. Consequently, after the formation of the MBs-Ab1-L. m complexes, the immunosensor (MnMOF-74@Ab2) was added to the matrices and made a sandwich hybrid (MBs@Ab1-L. m-Mn-MOF-74@Ab2). Afterward, the Mn^{2+} ions became free from the sandwich complex through the activity precipitated by H_2O_2. The free Mn^{2+} remarkably alters microelectrodes' impedance, resulting in ultrasensitive sensing of L. m. The DL by this procedure for L. m cells was 7.1 and 9.2 CFU/mL in water and milk, respectively. Similarly, Suo et al. prepared an AuNPs/FeMOF-PEI-GO aptasensor with a linear sensing range of 5×10^{-10}–0.005 mg/L and a low DL of 2.17×10^{-10} mg/L to detect patulin (PAT) in apple juice with trustworthiness, effectiveness, and high stability, providing a powerful technique for sensing trace patulin accurately [63].

In another study, Deep et al. modified screen-printed carbon electrodes with a nanocomposite containing zirconium-based MOF (UiO-66) and MoS_2 quantum dots covered with monoclonal antibodies specified for impedimetric and voltammetric sensing of aflatoxin M1 (AFM1) in milk samples [64]. Analysis recognized AFM1 within the concentration range of 0.21–6.0×10^{-5} mg/L with a DL of 6.0×10^{-5} mg/L and high sensitivity. Zare et al. also presented a label-free EC aptasensor for the detection of aflatoxin M1 in milk samples using PtNPs/MIL-101(Fe) [65]. The aptasensor presented a linear calibration range from 1.0×10^{-2} to 80.0 ng mL^{-1} and a DL of 2.0×10^{-3} ng mL^{-1} toward aflatoxin M1, with applicability in both powdered and pasteurized milk samples.

To recognize aflatoxin B1 (AFB1) in real samples of rice flour, Zare et al. prepared an aptasensor by decorating gold nanoparticles on the surface of Ni-MOF. The AFB1 aptamer was subsequently integrated onto the AuNPs/Ni-MOF, followed by coupling with the complementary DNA (cDNA). An electroactive probe, p-biphenol (PBP), was also interpolated inside the cDNA–aptamer twofold. The variation in EC feedback of inserted PBP in the presence or absence of AFB1 with the fixed aptamer was interpreted as an analytical response. They also synthesized a Cu MOF to monitor AFB1 in wheat flour [66]. The performance of the aptasensor was evaluated through voltammetric and impedimetric procedures utilizing Ferri/ferrocyanide as a redox indicator. The obtained detection range of this aptasensor was from 1.0×10^{-6} mg/L to 0.2 mg/L with a LOD of 8.3×10^{-7} mg/L.

Zhang et al. prepared an immunosensor based on a CoFe-MOFs/Gr/Chitosan (CS)/AuNPs hybrid to sense Salmonella in milk samples [67]. A bond formed between the amino functional group of the antibody and AuNPs resulted in the immobilization of specific antibodies on the electrode. A nitrogen absorption test was employed to study the surface area of related materials. The obtained surface areas of graphene, CoFe-MOFs, and CoFe-MOFs-graphene were 23.82, 24.27, and 15.11 m^2 g^{-1}, respectively. This result implies that the surface area of the obtained CoFe-MOFs-graphene decreases after graphene and CoFe-MOFs are compounded, probably because the CS contained in the solution blocks the pore size. CV was carried out to study the electrochemical behavior of modified electrodes in a phosphate bafer solution containing $[Fe(CN)_6]^{3-/4-}$. As expected, the peak current of CoFe-MOFs-graphene was higher than those of Gr and CoFe-MOFs, owing to the synergistic catalytic effect of CoFe-MOFs and Gr. In the composites, graphene acts as a conductive matrix to solve transfer charge barriers and compensate the conductivity defects of CoFeMOFs. The fabricated immunosensor sensed Salmonella within a linearity range of 2.4 × 102 CFU/mL to 2.4 × 108 CFU/mL and a DL of 1.2 × 102 CFU/mL. In another study, a multivariate titanium MOF utilized two different ligands of polyether

polymer and 1,4-benzene dicarboxylic acid for sensing zearalenone (ZEN) in peanut beer and corn [68]. In comparison with Ti-MOFs prepared by the single ligand, this multilayered morphology displayed higher bio-affinity toward the aptamer, with an ultralow DL in fg mL^{-1} level as well as a linearity of 10 fg mL^{-1}–10 ng mL^{-1}.

Iron-based MOF, NH_2-MIL-101(Fe), was treated with various quantities of cobalt phthalocyanine (CoPc) to prepare a set of NH_2-MIL-101(Fe)@CoPc nanohybrids introduced by Zhang et al. [69]. The active sites of Fe and Co could coordinate with the Nitrogen atoms in the aptamer, resulting in higher stability. Additionally, total covering of the electrochemically active centers of composites by aptamers simplified the fabrication process due to the lack of a requirement for extra blocking agents. These NH_2-MIL-101 (Fe)@CoPc nanocomposites were then utilized to assemble an impedimetric aptasensor to determine ochratoxin A (OTA) with reliable applicability to the analysis of the fresh watermelon juice and wine samples. The DL obtained via this EC biosensing strategy was 0.063 fg·mL^{-1} within the OTA quantity of 0.0001–100 pg·mL^{-1}

2.4. Pesticide Residues

Pesticides are defined as every chemical or organism employed to control, eliminate, repel, or reduce the impact of a pest. Since they are the most utilized products in the agri-food industry, the major problem with them is their accumulation in the food chain [70]. In the European Union, the Maximum Residual Limits (MRLs) authorized by the law are 0.1 µg/L for each pesticide and 0.5 µg/L for the total [71]. Therefore, it is necessary to strictly control and monitor them in the food chain, from water and soil to human bodies.

Li and coworkers proposed a single-pot self-assembly procedure to prepare encapsulated methylene blue (MB) ZIF-8 composites. [72]. In their designed system, ZIF-8 acts as the host, and MB is an electroactive molecule to produce the EC signal. This fabricated system also contained acetylcholinesterase enzyme (AChE) and acetylcholine (Ach) as recognition components. In the absence of a pesticide, ACh was hydrolyzed by AChE, which changed the environment's acidity, collapsing the ZIF-8/MB hybrid and creating a strong diffusion current from free MB. Instead, in the presence of pesticide, the action of AChE was hindered, leading to the maintenance of the ZIF-8/MB structure without releasing MB molecules. Therefore, as a result of "locked" MB molecules, the produced signal would be very weak. The proposed procedure was capable of sensitively monitoring organophosphates (Ops) with a relatively low DL and was applicable for the analysis of the real samples of Apple and Eggplant. Kushwaha et al. also proposed an EC Mn/Fe MOF-based platform for sensing OP pesticides [73]. The hetero-metal synergism between the Mn^{2+} and Fe^{3+} ions was employed for the electro-determination of chlorpyrifos. In another work, Cheong et al. prepared Burkholderia cepacia lipase (BCL)@MOF biosensors for fast, reliable, and direct detection of methyl parathion residues in vegetables [7]. The mesoporous structure simplified enzyme encapsulation and inhibited enzyme aggregation or leaching.

Due to the inert nature of Zr^{4+}, the redox characteristics of Zr-based MOFs like UiO-66 are limited. Bagheri and coworkers prepared Ce-doped UiO-66 to overcome these limitations and the practical detection of paraoxon in cabbage and spinach [74]. Ce has a satisfactory redox feature between the oxidation/reduction states of Ce^{3+}/Ce^{4+} and intensified electron transfer, along with much higher oxophilicity in comparison with Zr, which provides easier enzyme incorporation. This designed matrix was applied for immobilizing AChE to measure paraoxon concentration, which exhibited high sensitivity, a broad linear range, and low DL. Electrochemical evaluations by DPV in the absence and presence of ATCl were carried out. In the presence of ATCl, recognizable visible peaks were observed, attributed to the oxidation of the produced thiocholine by the hydrolysis of ATCl catalyzed by AchE, and the peak currents increased in the following order: AChE/Ce/UiO-66@MWCNTs > AChE/Ce/UiO66@CB > AChE/Ce/UiO-66@GO > AChE/Ce/UiO-66 > AChE/UiO-66. The anodic peaks observed by CV showed linearity that increased with the scan rate, representing a surface-controlled process. This observation is explained as

follows: The AChE has two anionic and cationic sites, and the carbonyl site of the ATCl interacts with the cationic site. After thiocholine production, the nitrogen of thiocholine with a positive charge binds to the anionic site of AChE, which justifies the surface-controlled process. Similarly, Zhao et al. employed UiO-66-NH_2 loaded with Cd^{2+} and Pb^{2+} for the simultaneous detection of triazophos (TRS) and thiacloprid (THD) [75]. The morphology of the structure obtained by SEM displayed an octahedron-like structure with a smooth surface and good dispersion. The pore size of 1.3 nm and the surface area of 1018 $m^2 \cdot g^{-1}$, calculated using the BET equation, indicate a porous structure with a high surface area for nanoparticles, which are particularly attractive for metal ion adsorption. The capacity of the designed system for real analysis was evaluated by a spiked test in brown rice, which exhibited a broad linear range from 0.2 to 750 $ng \cdot mL^{-1}$, a desirable recovery of 84.6–92.6%, and DLs of 0.07 and 0.1 $ng \cdot mL^{-1}$ for TRS and THD, respectively.

With the benefits of biosensing technology, various biomolecules such as enzymes, antibodies, nucleic acids, and peptides have penetrated MOF-based EC platforms for direct and selective EC sensing of pesticides [76–78]. Gao et al. synthesized zirconium-based MOF nanocomposites (Pt@UiO66-NH_2) with uniformly dispersed Pt nanoparticles to provide stabilizing microenvironments for integration of acetylcholinesterase (AChE) to monitor organophosphorus pesticides (OPs) in real samples [79]. Due to the complementary effect of outstanding electron conductivity and high immobilizing sites, the fabricated biosensors displayed high sensitivity to malathion with a linear range from 1×10^{-14} M to 1×10^{-9} M and a DL of 4.9×10^{-15} M. The obtained biosensor could accurately detect the OP residuals in cabbage and apple samples. Basu and coworkers fabricated a layered surface based on the polyclonal antibody (rIgG) and gold nanoparticle (Chi-AuNP) joint with MOF [80]. The designed sensor could successfully recognize the four most popular pesticides, including Chlorpyrifos, Bifenthrin, Imidacloprid, and Dimethoate. However, it was unable to monitor Hexaconazole and Profenofos. This selective behavior is explained by the molecular sieve behavior of the MOF layer in addition to the receptor role of the rIgG and binding energy and length alteration for every pesticide. Analysis of real samples of vegetable extract confirmed the least interference from heavy metal ions, fast analysis, and good stability for the proposed system.

Hierarchical porous MOFs (HP MOFs) possess the benefits of both mesoporous/macroporous substances and microporous materials. These HP MOFs could provide fast mass/electron transfer, which helps improve EC performance [81,82]. For instance, Cheong and coworkers prepared a zeolitic imidazolate framework (ZIF) with hierarchical ordered macro-microporous morphology (MAC-ZIF-8) to encapsulate nano-Burkholderia cepacian lipase (nano BCL) [83]. The fabricated MAC-ZIF-8 had high crystallinity and thermal stability, which made it a great candidate to immobilize the nano-BCL. Although biocatalysts like lipase are usually unstable in severe reaction circumstances and cannot be recycled and reused, the nano-BCL@MAC-ZIF-8 demonstrated that they maintained their original configuration with great affinity to target and reuse for a successive hydrolysis reaction. The EC biosensors based on BCL@MAC-ZIF-8 were successfully employed for the determination of nitrogenous diphenyl ether pesticides (nitrofen) in real food samples of apricots. The obtained LOD was 0.46μM with a broad linearity range of 0−114 μM.

Wang et al. also proposed Cu-BTC MOFs with hierarchically structured structures for EC detection of Glyphosate in soybean and introduced new potential to sense non-electroactive chemicals [84]. An obvious redox related to the conversion of Cu^{2+}/Cu^{+} was observed at CuBTC/ITO by CV investigation. In comparison with a bare electrode, the response current of Cu-BTC in Cu-BTC/ITO was significantly enhanced. The response current of Cu-BTC/ITO was significantly reduced after treatment with glyphosate. This is because the Cu-BTC on the electrode reacts with glyphosate, resulting in a decrease in response current. It was found that the detection mechanism of Glyphosate strongly depends on the interaction of the chelating groups P=O, C=O, and N-H in glyphosate toward Cu^{2+}. Thus, to verify the selectivity of the designed sensor, four popular pesticides, including Trichlorfon (Tri), Carbendazim (Car), Acetochlor (Ace), and Thiram (Thi), were

chosen as the interference materials. The observations approved great anti-interference behavior for this sensor. This attitude was explained by the calculation of the free energy of [84] and Cu^{2+} via density functional theory (DFT). The calculation results exhibited that Thi, Tri, Car, and Ace hardly coordinate with Cu^{2+}, which was in agreement with the experimental findings.

2.5. Hydrogen Peroxide

Hydrogen peroxide (H_2O_2) is a vital oxidant with broad applications in different fields such as food processing, paper bleaching, sewage treatment, biotechnology, and the chemical industry. Some food industries employ H_2O_2 for sanitation, which undoubtedly results in the remaining H_2O_2 in their products. Investigations have proven that extra H_2O_2 is cytotoxic for living organs, leading to serious diseases, from metabolic disorders like diabetes to abnormalities in tissue like cancer. Thus, it is crucial to develop an accurate and user-friendly technique for selectively and sensitively monitoring H_2O_2. Recently, novel materials, such as MOFs and their composites, have been extensively utilized to design EC platforms for H_2O_2. For example, Park and coworkers synthesized an N-doped Co-MOF (N-Co-MOF) by using a Polyvinylpyrrolidone PVP-assisted procedure [85]. PVP was employed to provide a nitrogen source and play a surfactant role to inhibit agglomeration. The constructed electrode modified with N-Co-MOF exhibited a great DL of 0.04 μM with a broad linear range, high durability, and excellent selectivity toward H_2O_2 in the presence of usual interfering molecules such as oxalic acid (OA), CA, glucose (Glu), AA, and fructose (Fru). The actual testing of the sensor for tap water and lemon juice also provided satisfactory results.

According to the literature, Cu-MOFs have been considered encouraging substances for EC sensing platforms toward H_2O_2 determination for different reasons, including that, firstly, these Cu-contained frameworks obtain good catalytic performance for H_2O_2 because of the well-matched potential between Cu^+/Cu^{2+} redox peaks and H_2O_2 reduction. Additionally, the flower-like morphology of Cu-MOF provides an abundant active site, which facilitates H_2O_2 enrichment in the catalytic centers. To this end, Liu et al. fabricated the Cu-MOF/MXene as a nonenzymatic sensor for H_2O_2 determination [86]. In this sensor, the MXene plays both roles of conductivity improvement and electrostatic medium to immobilize a greater extent of Cu-MOFs on the electrode surface. As a proof-of-concept electrocatalytic activity of Cu-MOF, the CV of the CuMOF/ERGO4/ITO electrode was recorded. In the absence of H_2O_2, a reduction peak at −0.33 V was observed related to the reduction of Cu^{2+} to Cu^+. In the presence of H_2O_2, this reduction peak is clearly enhanced, indicating the high electrocatalytic reduction of H_2O_2 mediated by the metallic centers of Cu-MOF/ERGO. Finally, these composite promises excellent sensor selectivity in the complex matrix and was practically employed for the measurement of H_2O_2 in serum and milk samples. Yeap and coworkers also proposed Cu-MOF incorporated with Gr as non-enzymatic sensing of H_2O_2 in milk samples [87]. The comparison between the EC results obtained from the prepared ECS and some previously reported H_2O_2 sensors clearly demonstrated that the Cu-MOF/rGO electrode provided greater performance regarding DL, linearity range, and sensitivity for H_2O_2 determination. You and coworkers prepared two different morphologies of Cu-MOFs to compare and study the relationship between structure and electrocatalytic activity [88]. According to their investigations, the 3D Cu-MOFs had octahedral morphology and provided lower resistance with an intense response for the electrocatalysis of H_2O_2 reduction compared with the 2D Cu-MOF, confirming that the structure effectively impacts the EC activity. The electrode modified with 3D Cu-MOF presented two linearity ranges from 2 μM to 3 mM and 3 to 25 mM, and a DL of 0.68 μM. Moreover, the sensor was utilized for H_2O_2 sensing in milk samples, indicating acceptable applicability and prospects. The ultrathin 2D MOF nanosheets (Cu-TCPP)/multi-walled carbon nanotubes (MWCNTs) composite was developed by Cao and coworkers as a non-enzymatic ECS to monitor hydrogen peroxide (H_2O_2) [89]. The hybrid material was coated on the electrode through the Langmuir-Schäfer method, which provided a

multilayer film EC platform. According to their findings, MWCNTs incorporation enhanced electrical conductivity and increased sensor sensitivity. The designed sensor is applicable for the measurement and monitoring of H_2O_2 in actual samples such as beer with a DL of 0.70 μM, a high sensitivity of 157 μA cm^{-2} mM^{-1}, and superior selectivity and stability in comparison with previously existing natural enzyme-based or pure MOF-modified electrodes. Zeng et al. employed partial pyrolysis to prepare MOF/CuxO composites in a core-shell restructure [90]. As illustrated in Figure 1, under 350 °C pyrolysis temperatures, because of different thermal stabilities for HKUST-1 and ZIF-8, the CuxO nanoparticles were fabricated from HKUST-1 and distributed in the shell of ZIF-8. Owing to the synergetic effect of the sieving properties of ZIF-8 and the electrocatalytic feature of CuxO on H_2O_2, the CuxO@ZIF-8-modified electrode displayed a wide linear range of 1.5–21,442 μM and a low DL of 0.15 μM in H_2O_2 detection. Additionally, as a result of the suitable size and shape of ZIF-8, the H_2O_2 molecules can diffuse through the shell while other larger molecules are not capable of entering, resulting in the hybrid substance displaying high selectivity toward H_2O_2.

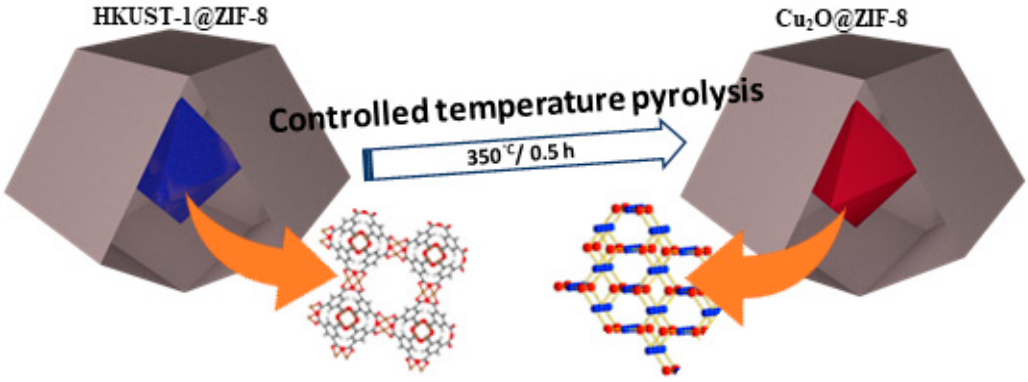

Figure 1. Schematically transformation of HKUST-1@ZIF-8 into Cu_xO NPs@ZIF-8.

Kung and coworkers electrochemically deposited cobalt within the pore of zirconium-based MOF (MOF-808) crystals [91]. This stepwise electro-preparation method could assist the formation inside the nano-area of the thin-film substrate, leading to a higher extent of cobalt cramped in the MOF pores. Since Zr-MOFs have high stability in acidic or neutral aqueous environments, the MOF morphology would remain undamaged during both electro-fabrication and EC sensing. Moreover, the rigid MOF could inhibit the aggregation of cobalt during the EC detection process. Using the amperometry technique for H_2O_2 determination, the sensitivity, the DL, and the linearity range of 382.27 mA/mMcm^2, 1.3 mM, and 10–450 mM were obtained, respectively.

Abraham and his coworker prepared a selective and sensitive platform for the measurement of H_2O_2 at biological pH utilizing AgNPs integrated zinc-MOF (AgNPs-Zn-MOF) [92]. Here, the Zn-MOF was performed as a matrix for AgNP loading. Further, according to impedance tests, the AgNPs resulted in higher conductivity and a faster electron transfer rate than bare Zn-MOF. The practical investigations of the AgNPsZn-MOF electrode for monitoring the extent of H_2O_2 in milk, human serum, and urine approved the potential ability of synthesized hybrid substances for real sample analysis.

The preservation effect of MOF presents excellent stability for fixing enzymes. However, in comparison with a free enzyme, the small pores of MOFs may reduce the availability and performance of the integrated enzyme. To solve such an issue, Ge and coworkers prepared ZIF-8 with both meso and micropores for Cytochrome c (Cyt c) incorporation to detect H_2O_2 in food samples of milk and beer [93]. This morphology provides an opportunity for immobilized Cyt c to display higher affinity to the substrate than bare Cyt c, resulting in approximately 128% raised enzymatic activity and 1.4- times more sensitivity for EC determination of H_2O_2. The response of Cyt c@mesoZIF-8 toward H_2O_2 was exten-

sively greater than the response to Glu, dopamine (DA), and bovine serum albumin (BSA), confirming good selectivity.

Some π-conjugated aromatic hydrocarbons, including 2,3,6,7,10,11-hexaiminotriphenylene (HITP), 2,3,6,7,10,11-hexahydroxytriphenylene (HHTP), and benzenehexol (HOB), have the potential to cooperate with metals and influence the conduction process [94]. The existent π-π interaction also simplifies charge transfer both in-bond and in-space. Exploiting this property, Zhang et al. fabricated a 2D conductive MOF with numerous nanosized channels. A single-layer nanosheet was prepared via the Langmuir Blodgett (LB) technique at the water-air interface. The interaction between Co and O decreased the energy inconsistency and enabled charge movement and electron conduction. Additionally, the counterion pair originated from electrostatic interactions, resulting in easier electronic orientation and movement. Interestingly, the porous morphology for proton transfer and the available metal spots provided the 3-layer structure with outstanding reducibility toward H_2O_2 with a DL of 3.08 nM.

2.6. Antibiotic Residue

Antibiotic discovery is considered a critical point in scientific history, however, the extravagance of antibiotics gave rise to not only the rising bacteria's antimicrobial resistance but also the accretion in farming products that has endangered the safety of food and, consequently, human health [95]. Thus, as an effort, nanostructured EC sensing containing various nano-substances have frequently been employed to monitor antibiotic residues [96]. Aptamers are a short sequence of artificial DNA or RNA with the ability to specifically bind to a complementary molecule. Recently, some researchers have been reported to have developed aptamers in sensing technology, so aptamer biosensors (aptasensors) have become one of the most popular nucleic acid-based sensors [97]. Liu and coworkers introduced Co-MOF on Covalent Organic Framework (COF) to make a hybrid structure as a matrix for immobilization of an aptamer to be employed as a label-free aptasensor for ampicillin (AMP) measurement [98]. The aptamer integration was carried out via bio-affinity between the aptamer and the Co-MOF@TPN-COF substrate through π-π stacking and hydrogen binding. The EC investigation for this aptasensor using the EIS technique obtained a DL of 0.217 fg mL^{-1} with linearity from 1.0 fg mL^{-1} to 2.0 ng mL^{-1}. The applicability of the designed sensor was also evaluated for the analysis of milk, river water, and human serum samples, which successfully displayed great potential for practical use.

Du et al. reported two immunosensors fabricated from two Al-based MOFs containing the linker 4,4′,4″-nitrilotribenzoic acid (NTB) to monitor and measure vomitoxin and salbutamol (SAL) in wine and pork samples [99]. In comparison with divalent d-block metal-based MOFs (specifically Zn^{2+} or Cu^{2+}), the trivalent f-block lanthanides of Al^{3+}-based MOFs were confirmed to exhibit high thermal or physicochemical stability. Their findings displayed appropriate anti-interference ability even in a complex environment for the proposed EC immunosensor. They also developed a bimetallic CoNi-MOF using the mixed organic linkers of 4-(1H-tetrazole-5-yl)benzoic acid (H_2TZB) and 2,4,6-tri(4-pyridyl)-1,3,5-triazine (TPT) [100]. As a result of the $\pi-\pi^*$ stacking and electrostatic forces between carboxyl groups from H_2TZB and amino groups from antibodies, the antibodies can be connected onto MOF to fabricate an immunosensor, specifically for the detection of deoxynivalenol (DON) or SAL (schematically shown in Figure 2). The constructed immunosensor exhibited high sensitivity with low DLs of 0.05 and 0.30 pg·mL^{-1} for DON and SAL detection, respectively, and a linearity of 0.001 to 0.5 ng·mL^{-1}. Real sample evaluation demonstrated the potential of the fabricated platform to recognize target substances in milk and pork, with high selectivity in the presence of other interferences.

An impedimetric aptasensor using a Ce-based-MOF@MCA composite was constructed for oxytetracycline (OTC) sensing in different aqueous environments, such as milk, wastewater, and urine [101]. In the presence of the target, the interacted aptamer-target was created, resulting in a conformational alteration in an aptamer that could inhibit redox probes' transportation to an electrode surface. This phenomenon led to a reduction in

the impedimetric signal (signal off). Another impedimetric aptasensor for the sensing of penicillin in milk samples was constructed by Du and coworkers based on two Ag^+-based MOFs with different counter anions (SiF_6 and CH_3SO_3) using tri(pyridine-4-yl)amine (TPA) and Ag^+ salts in ambient conditions [102]. Importantly, the activity of the designed aptasensor can be exceptionally adjusted through anion changes in the isostructural MOFs since every anion interacts differently with aptamers. Both MOF materials displayed great EC performance for determining penicillin in ultra-trace concentrations. Remarkably, the lowest obtained DL was 0.849 pg mL^{-1} in a linear range between 0.001 and 0.5 ng mL^{-1}, and the sensor could correctly detect penicillin in a raw milk sample.

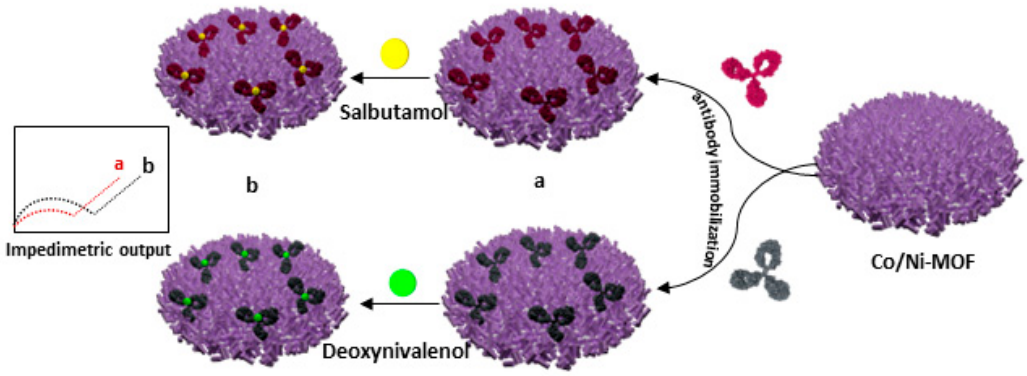

Figure 2. Schematic exhibition of the bimetallic MOF-based immunosensor for sensing deoxynivalenol and salbutamol.

Fabrication of EC aptasensors for Enrofloxacin (ENR) determination was carried out by Du et al. [103]. In their research, the synthesized bimetallic MOF displayed good electrical conductivity, determined as 1.46×10^{-2} S·cm^{-1}, which was owing to the in-plane full charge mobility within the repeating π-conjugated structure in the Gr-like sheets, high-energy electrons or holes, and well-organized π−π stacking interactions. The electrocatalytic activity toward redox reactions of ENR leads to a low DL of 0.2 fg·mL^{-1} with great selectivity, reproducibility, and applicability in milk sample analysis.

Enzyme-assisted target recycling amplification (TRCA) is one of the intensifying techniques that contains the assimilation of the aptamer by an exonuclease (Exo I). This method was used to detect streptomycin (STR) employing $Ru(NH_3)_6^{3+}$ (RuHex) as the redox probe by Sun et al. [104]. The electrode surface was easily covered by a mixed monolayer of thiolated dsDNA and 6-mercapto-1-hexanol (MCH) on Au. While the STR was not present, the Exo I would not digest the fabricated dsDNA. As soon as STR existed, it could combine with its aptamer in dsDNA to fabricate the aptamer-STR connection with the availability of the 3′ end and make the aptamer free from dsDNA. Consequently, the enzyme Exo I digested the aptamer in the aptamer-STR complex from its 3′-end, resulting in the target becoming free to start new cycles of complexation with other aptamers. Afterward, the MOFs integrated with aptamers of anti-streptomycin were introduced onto the electrode. The MOF-aptamers were connected to the free cDNA on the surface of the electrode. In the end, many aptamers tied to the MOFs captivated RuHex and added to the environment. A high-produced signal (signal on) was recorded by DPV. A dual intensification of the response was produced owing to target recycling amplification (TRCA) and the employment of MOFs-bio bar codes (dsDNA fabricated through hybridizing the aptamer with a cDNA).

2.7. Antioxidant Compounds

Antioxidants are healthy compounds that exist primarily in natural or manufactured forms. Since natural antioxidants are valuable for human health and could perform a critical role in the inhibition and treatment of different diseases, including myocardial infarction, cancer, and oxidative stress, they attract great attention in various areas like

food chemistry and medical care. Among the natural compounds that exist in fruits and herbs, Polyphenolics have been found to have a great influence on bitterness, acerbity, color, taste, scent, and oxidative durability in plant-based foods. So far, the determination of these antioxidants is usually performed through chromatographic methods, which require advanced instruments. Interestingly, according to the literature reports, the antioxidant characteristics of polyphenols are strongly dependent on their EC attitude. Blasco et al. introduced the antioxidant index as total phenolic content calculated via an EC procedure for the evaluation of the antioxidant quantity in crops. Thus, EC techniques with the benefits of analysis in complex matrices have recently received growing interest in this field. To achieve this aim, Wang and coworkers synthesized a methylene blue/flower-like nickel–terephthalic acid MOF nano-composite (MB@Ni–TPA MOF) and electropolymerized them to prepare a polymethylene blue/Ni–TPA MOF on an electrode to employ as a ratiometric sensor for the antioxidant index calculation in chrysanthemum tea [105]. The total polyphenolic content in chrysanthemum tea determined by this sensor was comparable to that achieved by Folin-Ciocalteu spectrophotometry. In another work, Guo et al. employed Zirconium-based MOF-($Zr\ 6O_4(OH)_4$(fumarate)$_6\cdot xH_2O$) and MC to prepare a composite [106]. The sensor based on MOF-801/MC could successfully detect GA and luteolin in green tea, with a broad linear range for GA monitoring from 0.2 to 100 μM and a high sensitivity of 44.363 μA μM^{-1} for luteolin. Exploiting the excellent stability of Zirconium-based MOF, they also prepared a bimetallic CuZr MOF with high stability in both acidic and basic media [107]. It is hypothesized that the magnificent performances of the composite are mainly attributed to various aspects: (A) The synergetic effect between Cu and Zr provides the higher activity. (B) The integration of rGO/MWCNTs not only facilitates overall charge transport but also effectively inhibits the conglomeration of MOF-818, leading to higher active sites. (C) The meso-macroporous morphology of the composite presented efficient channels for electrolyte transport, resulting in accelerated reaction kinetics. (D) The combination of these collaborations gives a higher response.

Various conventional electro-active MOFs, including Ni-MOF, Co-MOF, Cr-MOF, and Cu-MOF, have also been developed as electrode modifiers in designing nonenzymatic ECS for different antioxidants. Owing to their pleasant characteristics, these redox-active MOFs can effectively boost the response signals, consequently improving detection sensitivity. Among such electroactive MOFs, Huang et al. presented a novel sensor by integrating Cu-MOF (>2 μm) and Co-MOF (>30 μm) into an elastic device for nutrient investigation [108]. With the implementation of a flexible polyethylene therphetalate (PET) layer coated by small particle MOF with a microfluidic system, an ECS was constructed to detect some of the most critical antioxidants like ascorbic acid (AA), glycine, and L-tryptophan (L-Trp) with a detection limit (DL) of 14.97, 0.71, and 4.14 μM, respectively.

Caffeine (CAF), a natural polyphenol found in multiple herbs, specifically coffee, cocoa, and tea, performs well-known antioxidant activity in the human body. Up until now, different EC-modified systems have been proposed to determine the CAF accurately. For instance, Radhakrishnan and coworkers prepared a Cu-MOF/Gr composite to determine caffeine in tea and coffee samples [109]. The cyclic voltammograms recorded for caffeine at bare, and modified electrodes with Gr, Cu-MOF, and Cu-MOF/GE dispayed caffeine electro-oxidation peak currents of 175.3 μA, 198.9 μA, and 175.2 μA at bare, graphene oxide, and Cu-MOF, respectively. Further, the oxidation peak potential of Cu-MOF/graphene (1.40 V) is lower than that of bare GC (1.49 V), graphene oxide (1.50 V), and Cu-MOF (1.47 V) modified GCEs. This reduction in oxidation potential is influenced by two main parameters. (ii) The catalytic properties of CuMOF and the flower-like porous Cu-MOF structure. The modified electrode with composite exhibited good EC activity for caffeine oxidation, and the linear range of 5 mM to 450 mM with a DL of 1.38 mM, along with good selectivity, stability, and reproducibility, were obtained from a designed sensor.

CA and AA are two important weak organic acids that naturally exist in citrus fruits and are considered natural antioxidants. Traditional bare electrodes, such as Pt, Au, and glassy carbon, have been utilized to determine the AA, but due to the overpotential of

the vitamin C and the production of irreparable adsorbed chemicals, the electrode surface became foul, leading to unacceptable sensitivity and selectivity [110]. Thus, various nanomaterials have been employed to modify ordinary electrodes to reduce the overpotential and improve electrode performance. For example, Ramanujam et al. designed a modified electrode using Cobalt-Bipyridine MOF incorporated on CNT/Nafion for AA detection [111]. In this study, MOF played a role as a redox mediator, which displayed well-defined redox peaks attributed to the Co^{3+}/Co^{2+} and the MWCNTs performing both MOF immobilization and providing electrical conductivity for the substrate. formation of a complex between -SO3 $-$ and $[Co(bpy)_2NO_3]^+$ probably was in charge of AA monitoring. To test for the AA electrochemical oxidation on GCE/MWCNTs@Co-bpy/Nf, voltamogram was recorded in the absence and presence of AA. In the presence of AA, AA was oxidized at an onset potential of 0.08 V, and a steady state current of 13 μA was recorded at a potential >0.2 V. Comparison of this voltamogeram with those obtained by control electrodes, revealed a higher overpotential for AA oxidation at (>0.3 V) with lower current at control electrodes and the GCE/MWCNTs, although it oxidizes AA at a lower potential and is not selective to AA alone. Studying the reaction kinetics displayed that the anodic and cathodic peak currents increase with the log υ with a slop of 0.5, while the peak potential remains almost constant, indicating a diffusion-controlled process. According to their observations, the modified electrode displayed the great capability of AA detection in samples like beverages with acceptable tolerance to other popular interferants like CA, OA, SA, FA GL, FA, SU, and MA. Pang and coworkers prepared ultrathin nanosheet Ni-MOF through a controlled hydrothermal route [112]. This nanosheet Ni-MOF has also been confirmed to display catalytic behavior toward AA oxidation with high selectivity and an acceptable linear range from 0.5 μM to 8065.5 μM. Among MOFs, the MIL-101(Fe) has great attention for accessible cages and low framework density. Thus, Tashkhourian et al. employed Fe-based MOF (MIL-101) for the detection of CA [113]. According to the BET plot, the calculated surface area, total pore volume (p/p0 = 0.990), and mean pore diameter of MIL-101(Fe) were 290 $m^2\ g^{-1}$, 0.53 $cm^3\ g^{-1}$ and 7.35 nm, respectively. Based on the obtained results, this ECS displayed a surface-confined redox process with a proper linear range and good DL for monitoring CA in some commercial beverages.

Polyoxometalates (POMs) are a large group of distinct, mostly anionic polynuclear metal-oxo clusters, which are generally fabricated via the condensation of a metal oxide polyhedron (MOx)n, (M = Mo^{6+}, W^{5+} or V^{5+}, x = 4–7) [114]. The oxidation and reduction states of POMs are highly stable, and the numerous redox active sites empower them to be great candidates for electrocatalysis [115]. Freire and coworkers introduced the vanadium-substituted phosphomolybdate anion into Cr-base MIL-101(Cr) with the protection of each MOF and POM structure [116]. The surface coverage of the hybrid electrode is approximately ten times higher than that of each individual constituent electrode and displayed exceptional capacity in the simultaneous monitoring of AA and DA.

Flavonoids are bioactive polyphenolic materials presented in botanicals. As a natural flavonoid, Luteolin (LU), with a cis-diol configuration extracted from diverse plants, fruits, and vegetables, could play a therapeutic role in cough, irritation, and cardiac illness. Due to the recognition capability of LU by zirconium ions, the Zr-based MOF (UiO-66) has been introduced to recognize LU. However, to broaden the detection range and enhance the system's adsorption ability, the low conductivity problem needs to be solved. Thus, Liu and coworkers employed rGO and UiO-66 for modification of the electrode and application of the composite to the electrochemical sense of LU [117]. Under optimal circumstances, the modified electrode displayed an acceptable linear range and reproducibility. It could also accurately detect eight times testing for one electrode, which guaranteed the applicability of the designed system. Verification of the proposed sensor for a sample of chrysanthemums and hawthorn extracts displayed reliable results and confirmed the productivity of the composite.

Exploiting the good redox characteristics of Ni-based compounds, Qu et al. prepared a Ni-MOF on NiO nanosheet layer for electrochemical luteolin detection [118] luteolin

sensor provided a low DL of 3 pM, outstanding linearity from 0.01 nM to 1 nM and 1 nM to 50 µM with real applicability for truthful recognition of luteolin contents in commercial samples [112]. An ultrasensitive EC system for the investigation of glutathione (GSH) in various vegetable samples was developed utilizing the Au@Cu-MOF nanocomposite of Cu -MOF as a wrapping shell and encapsulated Au particles, which were synthesized through coordinate replication of a Cu_2O redox-template technique [119] (shown in Figure 3). The phenomenon called "crowding-out effect" in this ECS provided high selectivity, a broad linear range of 0.01–40 nM and 40 nM to 10 µM, and a DL of 2.5 pM for the designed sensor.

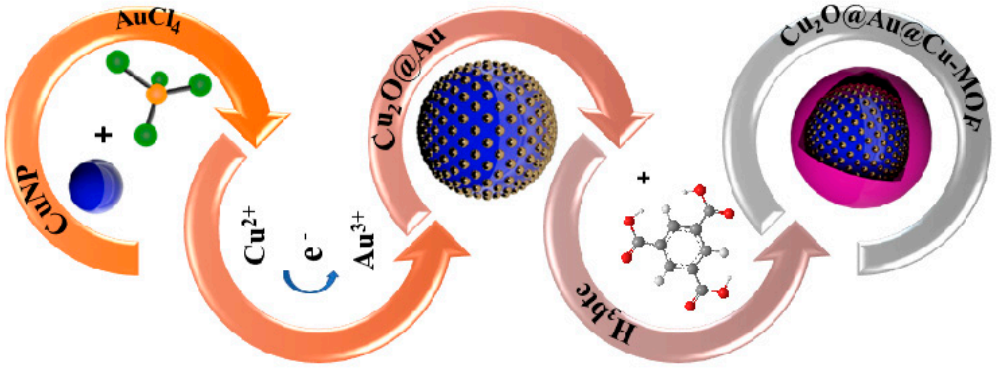

Figure 3. Schematically illustration of fabrication process of Au@CuMOF Nanocapsule.

3. Conclusions and Future Directions

In this review, we summarize recent developments in MOF-based EC sensing systems to evaluate various important factors in the food chain. Recently, the importance of food quality control has inspired many surveys to introduce relevant materials, feasible techniques, and truthful sensors. As discussed, MOF materials have presented exceptional characteristics and detection abilities when utilized in the fabrication of EC sensors for food quality control. Their unique porous morphology leads to a high inner detection region, their ordered structure presents the molecular sieve property, and their multiple active sites of ligands and metals provide an opportunity for modification and selective sensing. The provided overview of the research on MOF-based sensors illustrated the diversity of structures in this field. Table 1 outlines a general sketch of the reported MOF-based materials in electrochemical evaluations of food. Besides the vast potential of MOF to overcome its serious limitations as well as improve some of its analytical performance to be more sensitive, stable, and selective, different attempts have been carried out. For example, some researchers regulated the structure of MOFs using new preparation procedures or modification techniques to fabricate nanoscale MOFs with higher specific areas and better mass/electron transfer rates. The combination of MOFs with various conductive substances, including metal NPs, carbon nanomaterials, and polymers, has also been employed to improve conductivity. Additionally, two-dimensional MOF nanosheets have been introduced to enhance EC performance owing to the rapid charge transfer and higher accessibility of active sites originating from 2D structures. Moreover, for food safety evaluation in real samples, the anti-interference ability of MOF-based substances has been further refined through a novel functionalization process, which helps to sense specific analytes successfully. In conclusion, the majority of research confirmed that MOFs and MOF-based materials are effective in food safety sensors, and with the suitable design and incorporation of the different substances into MOF, pioneering studies in the future could result in MOF-based materials being extensively employed in the routine and online usage of EC sensing.

Table 1. General sketch of the reported MOF-based materials in electrochemical evaluations of food.

Number	Electrode Materials	Analyte	Electrochemical Method	Sensitivity	DL	Ref
1	GA/UiO-66-NH_2	Heavy Metals	Differential pulse stripping voltammetry (DPSV)	0.2716, 0.5242, 0.3604, 0.3242 (μA/μM) for (Cd^{2+}, Pb^{2+}, Cu^{2+}, Hg^{2+}) respectively	0.02 μM for Cd^{2+}, 1.5 nM for Pb^{2+}, 7 nM for Cu^{2+}, and 2 nM for Hg^{2+}	[35]
2	Cu-MOF	Hg^{2+}	Differential pulse voltammetry (DPV)	0.062 (μA/nM)	0.0633 nM	[36]
3	MWCNT/UiO-66-NH_2	Cd^{2+}	electrochemical impedance spectroscopy (EIS) and CV	0.11 (μA/μg L^{-1})	0.2 μg/L	[37]
4	NH2-MIL-53(Al)/PPy	Heavy Metals	DPV	0.21 μA/μg L^{-1}) for Pb^{2+} 0.1 (μA/μg L^{-1} for Cu^{2+}	0.315 μg L^{-1} and 0.244 μg L^{-1} for Pb^{2+} and Cu^{2+} respectively	[38]
5	DNA/(Fe-)n-MOF	Heavy Metals	DPV	1.16 (μA/nM)	0.02 nmol L1	[39]
6	Ca-MOF	Heavy Metals	anodic stripping voltammetry (ASV	0.3 μA/μg L	0.6 μg L^{-1}	[40]
7	DNA/Cu-MOF	Heavy Metals	DPV	0.99 (μA/M) for Hg^{2+}	4.8 fM	[42]
8	DNAzyme/porph@MOF	Heavy Metals	Square wave voltammetric (SWV)	2.67 (μA/M) for Pb^{2+}	5 pM	[43]
9	Ag/Cu-MOFs	Food additives	DPV	0.03 (μA/nM) for	2.2 nM	[47]
11	Fe-BTC	sunset yellow	DPV	0.02 (μA/nM) for.	0.015 nM	[49]
13	MWCNTs/Co-MOFs	nitrite	DPV	6.7 (μA/μM) for	18.8 μM	[51]
14	Cu-MOF	Nitrite	Amperometry	7.48 (μA/mM)	72 nM	[52]
15	rGO/Cu-TDPAT	nitrite	Amperometry and DPV	0.0096 and 0.0095 (μA/μM) by amperometry and DPV respectively	0.006 μmol·L^{-1}	[53]
16	3D structured DNA-PtNi@Co-MOF	(ZEN)	DPV	3 (μA/g mL^{-1}) for	1.37 fg/mL	[58]
17	cDNA/UiO-67-GR	S. typhimurium	DPV	3.12 (μA/CFU·mL^{-1})	5 CFU·mL^{-1}	[61]
18	Mn-MOF-74	Listeria monocytogens	EIS	1.378(Ω/CFU·mL^{-1})	7.1 CFU/mL	[62]
19	MoS_2/UiO-66	aflatoxin M1	EIS	1.27 (kΩ/ng mL^{-1}) for	0.06 ng mL^{-1}	[38]
20	ZIF-8/MB	Pesticide residue	DPV	0.2 (nA/ng mL^{-1}) ZIF-8/MB	1.7 ng/mL	[72]
21	Ce/UiO-66@MWCNTs	acetylthiocholine chloride	Amperometry	0.015 (μA/μM)	0.004 nM	[74]
22	Pt@UiO66-NH2	malathion	SWV	270 (μA/μM) for	4.9 × 10^{-15} M.	[79]
23	Chi-AuNP-rIgG-BSA/MOF-5	chlorpyrifos	CV	25.4 μA/ng Lcm^{-2}	4 (ngL^{-1})	[80]
24	MAC-ZIF-8	nitrofen	CV	0.03 (μA/μM)	0.46 μM	[83]
25	Cu-BTC	glyphosate	DPV	0.78 (μA/μM)	1.4 × 10^{-13} M	[84]
26	N-Co-MOF	hydrogen peroxide	Amperometry	0.03 (μA/μM)	0.072 μM	[85]
27	MXene/Cu-MOF	hydrogen peroxide	Amperometry	0.03 (μA/μM)	0.35 μmol/L	[86]
28	Cu-BTC-MOF/GO	hydrogen peroxide	Amperometry	0.02 (mA/mM)	0.44 μM	[87]
29	HKUST-1	hydrogen peroxide	CV	46.38 (μA/mM)	0.68 μM	[88]
30	2D Cu-TCPP/MWCNT	hydrogen peroxide	Amperometry	157 μA/$cm^{-2}mM^{-1}$	0.70 μM	[89]
31	$Cu_xO/Cu_3(BTC)_2$	hydrogen peroxide	Amperometry	178 (μA mM^{-1} cm^{-2})	0.15 μM	[90]
32	Co@MOF-808	hydrogen peroxide	Amperometry	382.27 (μA/mM-cm^2)	1.3 μM	[91]
33	AgNPs-Zn-MOF	hydrogen peroxide	DPV	0.03 (μA/μM)	67 nM	[92]
34	Cytochrome *c*/ZIF-8	hydrogen peroxide	Amperometry	3.84 (mA·M^{-1}·cm^{-2})	-	[93]
35	CoNi-MOF	SAL	EIS	01 kΩ/ng·mL^{-1}	0.30 pg·mL^{-1}	[100]
36	Ce-MOF@MCA	oxytetracycline	EIS	051 kΩ/ng·mL^{-1}	35.0 fM	[101]
37	Ag(I)-MOF	penicillin	EIS	3.69 kΩ/ng·mL^{-1}	0.849 pg mL^{-1}	[102]
38	$Co_xNi_{3-x}(HITP)_2$	enrofloxacin	EIS	4.46 kΩ/pg·mL^{-1}	0.2 fg·mL^{-1}	[103]
39	UiO-66-NH2	streptomycin	DPV	1.5 μA/ng mL^{-1}	2.6 pg mL^{-1}	[104]
40	MOF-801	luteolin	DPV	44.363 μA $μM^{-1}$	2.90 nM	[105]
41	MOF-818@RGO/MWCNTs	chlorogenic acid (CGA),	DPV	12.50 μA/μM	5.7 nM	[106]
42	Cu-MOF/Graphene	Caffeine	LSV	0.710 μA $μM^{-1}$ cm^{-2}	1.38 μM	[109]
43	MIL-101(Fe)	CA	DPV	0.67 μA·$μM^{-1}$·cm^{-2}	4.0 μM	[113]
44	UiO-66/ErGO	Luteolin	DPV		0.00075 μM	[117]
45	NiO@Ni-MOF	Luteolin	DPV	25.4 μA/μM	3 pM	[118]

Author Contributions: B.H. and M.L.R.-M. Conceptualization; B.H. Writing—Original Draft Preparation, M.L.R.-M. Writing—Review and Editing. All authors have read and agreed to the published version of the manuscript.

Funding: This research was funded by MINECO-FEDER Plan Nacional (PID2021-122365OB-100). Junta de Castilla y Leon-FEDER VA202P20. CLU-2019-04 and «Infraestructuras Red de Castilla y León (INFRARED)» UVA01. Plan Tractor En Materiales Avanzados Enfocado A Los Sectores Industriales Claves En Castilla Y León: Agroalimentario, Transporte, Energía Y Construcción (MA2TEC).

Institutional Review Board Statement: Not applicable.

Informed Consent Statement: Not applicable.

Data Availability Statement: Not applicable.

Acknowledgments: We appreciate the financial support of MINECO-FEDER Plan Nacional (PID2021-122365OB-100). Junta de Castilla y Leon-FEDER VA202P20. CLU-2019-04 and «Infraestructuras Red de Castilla y León (INFRARED)» UVA01. Plan Tractor En Materiales Avanzados Enfocado A Los Sectores Industriales Claves En Castilla Y León: Agroalimentario, Transporte, Energía Y Construcción (MA2TEC).

Conflicts of Interest: There are no conflict of interest to declare.

References

1. Wright, C. Analytical methods for monitoring contaminants in food—An industrial perspective. *J. Chromatogr. A* **2009**, *1216*, 316–319. [CrossRef] [PubMed]
2. Li, Z.; Xu, X.; Fu, Y.; Guo, Y.; Zhang, Q.; Zhang, Q.; Yang, H.; Li, Y. A water-stable luminescent metal–organic framework for effective detection of aflatoxin B1 in walnut and almond beverages. *RSC Adv.* **2019**, *9*, 620–625. [CrossRef] [PubMed]
3. Pechprasarn, S.; Ittipornnuson, K.; Jungpanich, T.; Pensupa, N.; Albutt, N. Surface plasmon biosensor platform for food industry. In *Applied Mechanics and Materials*; Trans Tech Publications Ltd.: Bäch, Switzerland, 2019; pp. 103–108.
4. Xing, G.; Sun, X.; Li, N.; Li, X.; Wu, T.; Wang, F. New Advances in Lateral Flow Immunoassay (LFI) Technology for Food Safety Detection. *Molecules* **2022**, *27*, 6596. [CrossRef] [PubMed]
5. Alikord, M.; Mohammadi, A.; Kamankesh, M.; Shariatifar, N. Food safety and quality assessment: Comprehensive review and recent trends in the applications of ion mobility spectrometry (IMS). *Crit. Rev. Food Sci. Nutr.* **2022**, *62*, 4833–4866. [CrossRef] [PubMed]
6. Špánik, I.; Machyňáková, A. Recent applications of gas chromatography with high-resolution mass spectrometry. *J. Sep. Sci.* **2018**, *41*, 163–179. [CrossRef]
7. Wang, Z.; Ma, B.; Shen, C.; Cheong, L.-Z. Direct, selective and ultrasensitive electrochemical biosensing of methyl parathion in vegetables using Burkholderia cepacia lipase@ MOF nanofibers-based biosensor. *Talanta* **2019**, *197*, 356–362. [CrossRef]
8. Zeng, L.; Peng, L.; Wu, D.; Yang, B. *Electrochemical sensors for food safety. Nutrition in Health and Disease–Our Challenges Now and Forthcoming Times*; BoD—Books on Demand: Norderstedt, Germany, 2018.
9. Curulli, A. Electrochemical biosensors in food safety: Challenges and perspectives. *Molecules* **2021**, *26*, 2940. [CrossRef]
10. Manikandan, V.S.; Adhikari, B.; Chen, A. Nanomaterial based electrochemical sensors for the safety and quality control of food and beverages. *Analyst* **2018**, *143*, 4537–4554. [CrossRef]
11. Lv, M.; Liu, Y.; Geng, J.; Kou, X.; Xin, Z.; Yang, D. Engineering nanomaterials-based biosensors for food safety detection. *Biosens. Bioelectron.* **2018**, *106*, 122–128. [CrossRef]
12. Kitagawa, S. Metal–organic frameworks (MOFs). *Chem. Soc. Rev.* **2014**, *43*, 5415–5418.
13. Kim, H.; Yang, S.; Rao, S.R.; Narayanan, S.; Kapustin, E.A.; Furukawa, H.; Umans, A.S.; Yaghi, O.M.; Wang, E.N. Water harvesting from air with metal-organic frameworks powered by natural sunlight. *Science* **2017**, *356*, 430–434. [CrossRef] [PubMed]
14. Dong, Z.; Sun, Y.; Chu, J.; Zhang, X.; Deng, H. Multivariate metal–organic frameworks for dialing-in the binding and programming the release of drug molecules. *J. Am. Chem. Soc.* **2017**, *139*, 14209–14216. [CrossRef]
15. Hosseinzadeh, B.; Nagar, B.; Benages-Vilau, R.; Gomez-Romero, P.; Kazemi, S.H. MOF-derived conformal cobalt oxide/C composite material as high-performance electrode in hybrid supercapacitors. *Electrochim. Acta* **2021**, *389*, 138657. [CrossRef]
16. Kazemi, S.H.; Hosseinzadeh, B.; Kazemi, H.; Kiani, M.A.; Hajati, S. Facile synthesis of mixed metal–organic frameworks: Electrode materials for supercapacitors with excellent areal capacitance and operational stability. *ACS Appl. Mater. Interfaces* **2018**, *10*, 23063–23073. [CrossRef] [PubMed]
17. Hira, S.A.; Nallal, M.; Rajendran, K.; Song, S.; Park, S.; Lee, J.-M.; Joo, S.H.; Park, K.H. Ultrasensitive detection of hydrogen peroxide and dopamine using copolymer-grafted metal-organic framework based electrochemical sensor. *Anal. Chim. Acta* **2020**, *1118*, 26–35. [CrossRef] [PubMed]
18. eun Kim, S.; Muthurasu, A. Metal-organic framework–assisted bimetallic Ni@ Cu microsphere for enzyme-free electrochemical sensing of glucose. *J. Electroanal. Chem.* **2020**, *873*, 114356. [CrossRef]
19. Xiang, X.; Pan, F.; Li, Y. Flower-like bismuth metal-organic frameworks grown on carbon paper as a free-standing electrode for efficient electrochemical sensing of Cd2+ and Pb2+ in water. *Eng. Sci.* **2018**, *3*, 77–83. [CrossRef]

20. Ye, Z.; Wang, Q.; Qiao, J.; Xu, Y.; Li, G. In situ synthesis of sandwich MOFs on reduced graphene oxide for electrochemical sensing of dihydroxybenzene isomers. *Analyst* **2019**, *144*, 2120–2129. [CrossRef]
21. Cheng, W.; Tang, X.; Zhang, Y.; Wu, D.; Yang, W. Applications of metal-organic framework (MOF)-based sensors for food safety: Enhancing mechanisms and recent advances. *Trends Food Sci. Technol.* **2021**, *112*, 268–282. [CrossRef]
22. Zhang, Z.; Lou, Y.; Guo, C.; Jia, Q.; Song, Y.; Tian, J.-Y.; Zhang, S.; Wang, M.; He, L.; Du, M. Metal–organic frameworks (MOFs) based chemosensors/biosensors for analysis of food contaminants. *Trends Food Sci. Technol.* **2021**, *118*, 569–588. [CrossRef]
23. Marimuthu, M.; Arumugam, S.S.; Jiao, T.; Sabarinathan, D.; Li, H.; Chen, Q. Metal organic framework based sensors for the detection of food contaminants. *TrAC Trends Anal. Chem.* **2022**, *154*, 116642. [CrossRef]
24. Hitabatuma, A.; Wang, P.; Su, X.; Ma, M. Metal-Organic Frameworks-Based Sensors for Food Safety. *Foods* **2022**, *11*, 382. [CrossRef] [PubMed]
25. Wang, J.; Li, D.; Ye, Y.; Qiu, Y.; Liu, J.; Huang, L.; Liang, B.; Chen, B. A Fluorescent Metal–Organic Framework for Food Real-Time Visual Monitoring. *Adv. Mater.* **2021**, *33*, 2008020. [CrossRef] [PubMed]
26. Lai, H.; Li, G.; Xu, F.; Zhang, Z. Metal–organic frameworks: Opportunities and challenges for surface-enhanced Raman scattering—A review. *J. Mater. Chem. C* **2020**, *8*, 2952–2963. [CrossRef]
27. Lyu, F.; Zhang, Y.; Zare, R.N.; Ge, J.; Liu, Z. One-pot synthesis of protein-embedded metal–organic frameworks with enhanced biological activities. *Nano Lett.* **2014**, *14*, 5761–5765. [CrossRef] [PubMed]
28. Chang, Y.; Lou, J.; Yang, L.; Liu, M.; Xia, N.; Liu, L. Design and Application of Electrochemical Sensors with Metal–Organic Frameworks as the Electrode Materials or Signal Tags. *Nanomaterials* **2022**, *12*, 3248. [CrossRef] [PubMed]
29. Mehta, J.; Bhardwaj, N.; Bhardwaj, S.K.; Kim, K.-H.; Deep, A. Recent advances in enzyme immobilization techniques: Metal-organic frameworks as novel substrates. *Coord. Chem. Rev.* **2016**, *322*, 30–40. [CrossRef]
30. Mao, Y.; Li, J.; Cao, W.; Ying, Y.; Hu, P.; Liu, Y.; Sun, L.; Wang, H.; Jin, C.; Peng, X. General incorporation of diverse components inside metal-organic framework thin films at room temperature. *Nat. Commun.* **2014**, *5*, 5532. [CrossRef] [PubMed]
31. Yu, J.; Mu, C.; Yan, B.; Qin, X.; Shen, C.; Xue, H.; Pang, H. Nanoparticle/MOF composites: Preparations and applications. *Mater. Horiz.* **2017**, *4*, 557–569. [CrossRef]
32. Kalaj, M.; Bentz, K.C.; Ayala, S., Jr.; Palomba, J.M.; Barcus, K.S.; Katayama, Y.; Cohen, S.M. MOF-polymer hybrid materials: From simple composites to tailored architectures. *Chem. Rev.* **2020**, *120*, 8267–8302. [CrossRef]
33. Rai, P.K.; Lee, S.S.; Zhang, M.; Tsang, Y.F.; Kim, K.-H. Heavy metals in food crops: Health risks, fate, mechanisms, and management. *Environ. Int.* **2019**, *125*, 365–385. [CrossRef]
34. Wang, L.; Peng, X.; Fu, H.; Huang, C.; Li, Y.; Liu, Z. Recent advances in the development of electrochemical aptasensors for detection of heavy metals in food. *Biosens. Bioelectron.* **2020**, *147*, 111777. [CrossRef]
35. Lu, M.; Deng, Y.; Luo, Y.; Lv, J.; Li, T.; Xu, J.; Chen, S.-W.; Wang, J. Graphene aerogel–metal–organic framework-based electrochemical method for simultaneous detection of multiple heavy-metal ions. *Anal. Chem.* **2018**, *91*, 888–895. [CrossRef]
36. Singh, S.; Numan, A.; Zhan, Y.; Singh, V.; Van Hung, T.; Nam, N.D. A novel highly efficient and ultrasensitive electrochemical detection of toxic mercury (II) ions in canned tuna fish and tap water based on a copper metal-organic framework. *J. Hazard. Mater.* **2020**, *399*, 123042. [CrossRef] [PubMed]
37. Wang, X.; Xu, Y.; Li, Y.; Li, Y.; Li, Z.; Zhang, W.; Zou, X.; Shi, J.; Huang, X.; Liu, C. Rapid detection of cadmium ions in meat by a multi-walled carbon nanotubes enhanced metal-organic framework modified electrochemical sensor. *Food Chem.* **2021**, *357*, 129762. [CrossRef]
38. Wang, N.; Zhao, W.; Shen, Z.; Sun, S.; Dai, H.; Ma, H.; Lin, M. Sensitive and selective detection of Pb (II) and Cu (II) using a metal-organic framework/polypyrrole nanocomposite functionalized electrode. *Sens. Actuators B Chem.* **2020**, *304*, 127286. [CrossRef]
39. Wang, X.; Yang, C.; Zhu, S.; Yan, M.; Ge, S.; Yu, J. 3D origami electrochemical device for sensitive Pb2+ testing based on DNA functionalized iron-porphyrinic metal-organic framework. *Biosens. Bioelectron.* **2017**, *87*, 108–115. [CrossRef]
40. Kokkinos, C.; Economou, A.; Pournara, A.; Manos, M.; Spanopoulos, I.; Kanatzidis, M.; Tziotzi, T.; Petkov, V.; Margariti, A.; Oikonomopoulos, P. 3D-printed lab-in-a-syringe voltammetric cell based on a working electrode modified with a highly efficient Ca-MOF sorbent for the determination of Hg (II). *Sens. Actuators B Chem.* **2020**, *321*, 128508. [CrossRef]
41. Zhang, X.; Jiang, Y.; Zhu, M.; Xu, Y.; Guo, Z.; Shi, J.; Han, E.; Zou, X.; Wang, D. Electrochemical DNA sensor for inorganic mercury (II) ion at attomolar level in dairy product using Cu (II)-anchored metal-organic framework as mimetic catalyst. *Chem. Eng. J.* **2020**, *383*, 123182. [CrossRef]
42. Zhang, X.; Zhu, M.; Jiang, Y.; Wang, X.; Guo, Z.; Shi, J.; Zou, X.; Han, E. Simple electrochemical sensing for mercury ions in dairy product using optimal Cu2+-based metal-organic frameworks as signal reporting. *J. Hazard. Mater.* **2020**, *400*, 123222. [CrossRef]
43. Zhang, X.; Huang, X.; Xu, Y.; Wang, X.; Guo, Z.; Huang, X.; Li, Z.; Shi, J.; Zou, X. Single-step electrochemical sensing of ppt-level lead in leaf vegetables based on peroxidase-mimicking metal-organic framework. *Biosens. Bioelectron.* **2020**, *168*, 112544. [CrossRef] [PubMed]
44. Petrakis, E.A.; Cagliani, L.R.; Tarantilis, P.A.; Polissiou, M.G.; Consonni, R. Sudan dyes in adulterated saffron (*Crocus sativus* L.): Identification and quantification by 1H NMR. *Food Chem.* **2017**, *217*, 418–424. [CrossRef] [PubMed]
45. Trasande, L.; Shaffer, R.M.; Sathyanarayana, S.; Lowry, J.A.; Ahdoot, S.; Baum, C.R.; Bernstein, A.S.; Bole, A.; Campbell, C.C.; Landrigan, P.J. Food additives and child health. *Pediatrics* **2018**, *142*, e20181410. [CrossRef] [PubMed]

46. Rovina, K.; Siddiquee, S. Analytical and advanced methods-based determination of melamine in food products. In *Nanobiosensors*; Elsevier: Amsterdam, The Netherlands, 2017; pp. 339–390.
47. Zhou, Y.; Li, X.; Pan, Z.; Ye, B.; Xu, M. Determination of malachite green in fish by a modified MOF-based electrochemical sensor. *Food Anal. Methods* **2019**, *12*, 1246–1254. [CrossRef]
48. Darabi, R.; Shabani-Nooshabadi, M.; Karimi-Maleh, H.; Gholami, A. The potential of electrochemistry for one-pot and sensitive analysis of patent blue V, tartrazine, acid violet 7 and ponceau 4R in foodstuffs using IL/Cu-BTC MOF modified sensor. *Food Chem.* **2022**, *368*, 130811. [CrossRef] [PubMed]
49. Ji, L.; Peng, L.; Chen, T.; Li, X.; Zhu, X.; Hu, P. Facile synthesis of Fe-BTC and electrochemical enhancement effect for sunset yellow determination. *Talanta Open* **2022**, *5*, 100084. [CrossRef]
50. Lv, R.; Sun, R.; Du, T.; Li, Y.; Chen, L.; Zhang, Y.; Qi, Y. Cu2+ modified Zr-based metal organic framework-CTAB-graphene for sensitive electrochemical detection of sunset yellow. *Food Chem. Toxicol.* **2022**, *166*, 113250. [CrossRef]
51. Salagare, S.; Shivappa Adarakatti, P.; Venkataramanappa, Y. Designing and construction of carboxyl functionalised MWCNTs/Co-MOFs-based electrochemical sensor for the sensitive detection of nitrite. *Int. J. Environ. Anal. Chem.* **2022**, *102*, 5301–5320. [CrossRef]
52. Liu, H.-Y.; Wen, J.-J.; Xu, H.-X.; Qiu, Y.-B.; Yin, Z.-Z.; Li, L.-H.; Gu, C.-C. Development of a copper-based metal organic electrode for nitrite sensing. *J. AOAC Int.* **2021**, *104*, 157–164. [CrossRef]
53. He, B.; Yan, D. Au/ERGO nanoparticles supported on Cu-based metal-organic framework as a novel sensor for sensitive determination of nitrite. *Food Control* **2019**, *103*, 70–77. [CrossRef]
54. Saeb, E.; Asadpour-Zeynali, K. A novel ZIF-8@ ZIF-67/Au core–shell metal organic framework nanocomposite as a highly sensitive electrochemical sensor for nitrite determination. *Electrochim. Acta* **2022**, *417*, 140278. [CrossRef]
55. Velusamy, V.; Arshak, K.; Korostynska, O.; Oliwa, K.; Adley, C. An overview of foodborne pathogen detection: In the perspective of biosensors. *Biotechnol. Adv.* **2010**, *28*, 232–254. [CrossRef] [PubMed]
56. Tauxe, R.V. Emerging foodborne pathogens. *Int. J. Food Microbiol.* **2002**, *78*, 31–41. [CrossRef] [PubMed]
57. Zhao, X.; Lin, C.-W.; Wang, J.; Oh, D.H. Advances in rapid detection methods for foodborne pathogens. *J. Microbiol. Biotechnol.* **2014**, *24*, 297–312. [CrossRef]
58. He, B.; Yan, X. Ultrasensitive electrochemical aptasensor based on CoSe2/AuNRs and 3D structured DNA-PtNi@ Co-MOF networks for the detection of zearalenone. *Sens. Actuators B Chem.* **2020**, *306*, 127558. [CrossRef]
59. Zhu, X.; Li, B.; Yang, J.; Li, Y.; Zhao, W.; Shi, J.; Gu, J. Effective adsorption and enhanced removal of organophosphorus pesticides from aqueous solution by Zr-based MOFs of UiO-67. *ACS Appl. Mater. Interfaces* **2015**, *7*, 223–231. [CrossRef] [PubMed]
60. Liu, Y.; Hou, W.; Xia, L.; Cui, C.; Wan, S.; Jiang, Y.; Yang, Y.; Wu, Q.; Qiu, L.; Tan, W. ZrMOF nanoparticles as quenchers to conjugate DNA aptamers for target-induced bioimaging and photodynamic therapy. *Chem. Sci.* **2018**, *9*, 7505–7509. [CrossRef] [PubMed]
61. Dai, G.; Li, Z.; Luo, F.; Ai, S.; Chen, B.; Wang, Q. Electrochemical determination of Salmonella typhimurium by using aptamer-loaded gold nanoparticles and a composite prepared from a metal-organic framework (type UiO-67) and graphene. *Microchim. Acta* **2019**, *186*, 620. [CrossRef]
62. Wang, S.; Zhu, X.; Meng, Q.; Zheng, P.; Zhang, J.; He, Z.; Jiang, H. Gold interdigitated micro-immunosensor based on Mn-MOF-74 for the detection of Listeria monocytogens. *Biosens. Bioelectron.* **2021**, *183*, 113186. [CrossRef]
63. Lu, X.; He, B.; Liang, Y.; Wang, J.; Jiao, Q.; Liu, Y.; Guo, R.; Wei, M.; Jin, H.; Ren, W. An electrochemical aptasensor based on dual-enzymes-driven target recycling strategy for patulin detection in apple juice. *Food Control* **2022**, *137*, 108907. [CrossRef]
64. Kaur, G.; Sharma, S.; Singh, S.; Bhardwaj, N.; Deep, A. Selective and Sensitive Electrochemical Sensor for Aflatoxin M1 with a Molybdenum Disulfide Quantum Dot/Metal–Organic Framework Nanocomposite. *ACS Omega* **2022**, *7*, 17600–17608. [CrossRef]
65. Jahangiri–Dehaghani, F.; Zare, H.R.; Shekari, Z. Measurement of aflatoxin M1 in powder and pasteurized milk samples by using a label–free electrochemical aptasensor based on platinum nanoparticles loaded on Fe–based metal–organic frameworks. *Food Chem.* **2020**, *310*, 125820. [CrossRef] [PubMed]
66. Jahangiri–Dehaghani, F.; Zare, H.R.; Shekari, Z. A non-label electrochemical aptasensor based on Cu metal–organic framework to measure aflatoxin B1 in wheat flour. *Food Anal. Methods* **2022**, *15*, 192–202. [CrossRef]
67. Feng, K.; Li, T.; Ye, C.; Gao, X.; Yang, T.; Liang, X.; Yue, X.; Ding, S.; Dong, Q.; Yang, M. A label-free electrochemical immunosensor for rapid detection of salmonella in milk by using CoFe-MOFs-graphene modified electrode. *Food Control* **2021**, *130*, 108357. [CrossRef]
68. Duan, F.; Rong, F.; Guo, C.; Chen, K.; Wang, M.; Zhang, Z.; Pettinari, R.; Zhou, L.; Du, M. Electrochemical aptasensing strategy based on a multivariate polymertitanium-metal-organic framework for zearalenone analysis. *Food Chem.* **2022**, *385*, 132654. [CrossRef]
69. Song, Y.; He, L.; Zhang, S.; Liu, X.; Chen, K.; Jia, Q.; Zhang, Z.; Du, M. Novel impedimetric sensing strategy for detecting ochratoxin A based on NH2-MIL-101 (Fe) metal-organic framework doped with cobalt phthalocyanine nanoparticles. *Food Chem.* **2021**, *351*, 129248. [CrossRef] [PubMed]
70. Pérez-Fernández, B.; Costa-García, A.; Muñiz, A.d.l.E. Electrochemical (bio) sensors for pesticides detection using screen-printed electrodes. *Biosensors* **2020**, *10*, 32. [CrossRef]
71. Authority, E.F.S.; Bellisai, G.; Bernasconi, G.; Brancato, A.; Cabrera, L.C.; Castellan, I.; Ferreira, L.; Giner, G.; Greco, L.; Jarrah, S. Targeted review of maximum residues levels (MRLs) for indoxacarb. *EFSA J.* **2022**, *20*, e07527.

72. Li, X.; Gao, X.; Gai, P.; Liu, X.; Li, F. Degradable metal-organic framework/methylene blue composites-based homogeneous electrochemical strategy for pesticide assay. *Sens. Actuators B Chem.* **2020**, *323*, 128701. [CrossRef]
73. Janjani, P.; Bhardwaj, U.; Gupta, R.; Kushwaha, H.S. Bimetallic Mn/Fe MOF modified screen-printed electrodes for non-enzymatic electrochemical sensing of organophosphate. *Anal. Chim. Acta* **2022**, *1202*, 339676. [CrossRef]
74. Mahmoudi, E.; Fakhri, H.; Hajian, A.; Afkhami, A.; Bagheri, H. High-performance electrochemical enzyme sensor for organophosphate pesticide detection using modified metal-organic framework sensing platforms. *Bioelectrochemistry* **2019**, *130*, 107348. [CrossRef] [PubMed]
75. Yang, Y.; Cheng, J.; Wang, B.; Guo, Y.; Dong, X.; Zhao, J. An amino-modified metal-organic framework (type UiO-66-NH2) loaded with cadmium (II) and lead (II) ions for simultaneous electrochemical immunosensing of triazophos and thiacloprid. *Microchim. Acta* **2019**, *186*, 101. [CrossRef] [PubMed]
76. Felix, F.S.; Angnes, L. Electrochemical immunosensors—A powerful tool for analytical applications. *Biosens. Bioelectron.* **2018**, *102*, 470–478. [CrossRef] [PubMed]
77. Du, Y.; Jia, X.; Zhong, L.; Jiao, Y.; Zhang, Z.; Wang, Z.; Feng, Y.; Bilal, M.; Cui, J.; Jia, S. Metal-organic frameworks with different dimensionalities: An ideal host platform for enzyme@ MOF composites. *Coord. Chem. Rev.* **2022**, *454*, 214327. [CrossRef]
78. Toh, S.Y.; Citartan, M.; Gopinath, S.C.; Tang, T.-H. Aptamers as a replacement for antibodies in enzyme-linked immunosorbent assay. *Biosens. Bioelectron.* **2015**, *64*, 392–403. [CrossRef]
79. Ma, L.; He, Y.; Wang, Y.; Wang, Y.; Li, R.; Huang, Z.; Jiang, Y.; Gao, J. Nanocomposites of Pt nanoparticles anchored on UiO66-NH2 as carriers to construct acetylcholinesterase biosensors for organophosphorus pesticide detection. *Electrochim. Acta* **2019**, *318*, 525–533. [CrossRef]
80. Bhardwaj, R.; Rao, R.P.; Mukherjee, I.; Agrawal, P.K.; Basu, T.; Bharadwaj, L.M. Layered construction of nano immuno-hybrid embedded MOF as an electrochemical sensor for rapid quantification of total pesticides load in vegetable extract. *J. Electroanal. Chem.* **2020**, *873*, 114386.
81. Chen, X.; Zhang, Q. Recent advances in mesoporous metal-organic frameworks. *Particuology* **2019**, *45*, 20–34. [CrossRef]
82. Liu, D.; Zou, D.; Zhu, H.; Zhang, J. Mesoporous metal–organic frameworks: Synthetic strategies and emerging applications. *Small* **2018**, *14*, 1801454. [CrossRef]
83. Cheng, Y.; Ma, B.; Tan, C.-P.; Lai, O.-M.; Panpipat, W.; Cheong, L.-Z.; Shen, C. Hierarchical macro-microporous ZIF-8 nanostructures as efficient nano-lipase carriers for rapid and direct electrochemical detection of nitrogenous diphenyl ether pesticides. *Sens. Actuators B Chem.* **2020**, *321*, 128477. [CrossRef]
84. Cao, Y.; Wang, L.; Shen, C.; Wang, C.; Hu, X.; Wang, G. An electrochemical sensor on the hierarchically porous Cu-BTC MOF platform for glyphosate determination. *Sens. Actuators B Chem.* **2019**, *283*, 487–494. [CrossRef]
85. Hira, S.A.; Annas, D.; Nagappan, S.; Kumar, Y.A.; Song, S.; Kim, H.-J.; Park, S.; Park, K.H. Electrochemical sensor based on nitrogen-enriched metal–organic framework for selective and sensitive detection of hydrazine and hydrogen peroxide. *J. Environ. Chem. Eng.* **2021**, *9*, 105182. [CrossRef]
86. Cheng, D.; Li, P.; Zhu, X.; Liu, M.; Zhang, Y.; Liu, Y. Enzyme-free Electrochemical Detection of Hydrogen Peroxide Based on the Three-Dimensional Flower-like Cu-based Metal Organic Frameworks and MXene Nanosheets. *Chin. J. Chem.* **2021**, *39*, 2181–2187. [CrossRef]
87. Golsheikh, A.M.; Yeap, G.-Y.; Yam, F.K.; San Lim, H. Facile fabrication and enhanced properties of copper-based metal organic framework incorporated with graphene for non-enzymatic detection of hydrogen peroxide. *Synth. Met.* **2020**, *260*, 116272. [CrossRef]
88. Guo, X.; Lin, C.; Zhang, M.; Duan, X.; Dong, X.; Sun, D.; Pan, J.; You, T. 2D/3D Copper-Based Metal-Organic Frameworks for Electrochemical Detection of Hydrogen Peroxide. *Front. Chem.* **2021**, *9*, 743637. [CrossRef]
89. Wang, C.; Huang, S.; Luo, L.; Zhou, Y.; Lu, X.; Zhang, G.; Ye, H.; Gu, J.; Cao, F. Ultrathin two-dimension metal-organic framework nanosheets/multi-walled carbon nanotube composite films for the electrochemical detection of H_2O_2. *J. Electroanal. Chem.* **2019**, *835*, 178–185. [CrossRef]
90. Yang, J.; Ye, H.; Zhao, F.; Zeng, B. A novel Cu x O nanoparticles@ ZIF-8 composite derived from core–shell metal–organic frameworks for highly selective electrochemical sensing of hydrogen peroxide. *ACS Appl. Mater. Interfaces* **2016**, *8*, 20407–20414. [CrossRef] [PubMed]
91. Chang, Y.-S.; Li, J.-H.; Chen, Y.-C.; Ho, W.H.; Song, Y.-D.; Kung, C.-W. Electrodeposition of pore-confined cobalt in metal–organic framework thin films toward electrochemical H_2O_2 detection. *Electrochim. Acta* **2020**, *347*, 136276. [CrossRef]
92. Arul, P.; John, S.A. Silver nanoparticles built-in zinc metal organic framework modified electrode for the selective non-enzymatic determination of H_2O_2. *Electrochim. Acta* **2017**, *235*, 680–689. [CrossRef]
93. Zhang, C.; Wang, X.; Hou, M.; Li, X.; Wu, X.; Ge, J. Immobilization on metal–organic framework engenders high sensitivity for enzymatic electrochemical detection. *ACS Appl. Mater. Interfaces* **2017**, *9*, 13831–13836. [CrossRef]
94. Zhang, T.; Zheng, B.; Li, L.; Song, J.; Song, L.; Zhang, M. Fewer-layer conductive metal-organic Langmuir-Blodgett films as electrocatalysts enable an ultralow detection limit of H_2O_2. *Appl. Surf. Sci.* **2021**, *539*, 148255. [CrossRef]
95. Joshi, A.; Kim, K.-H. Recent advances in nanomaterial-based electrochemical detection of antibiotics: Challenges and future perspectives. *Biosens. Bioelectron.* **2020**, *153*, 112046. [CrossRef] [PubMed]

96. Khoshbin, Z.; Verdian, A.; Housaindokht, M.R.; Izadyar, M.; Rouhbakhsh, Z. Aptasensors as the future of antibiotics test kits-a case study of the aptamer application in the chloramphenicol detection. *Biosens. Bioelectron.* **2018**, *122*, 263–283. [CrossRef] [PubMed]
97. Vashist, S.K.; Luong, J.H. *Handbook of Immunoassay Technologies: Approaches, Performances, and Applications*; Academic Press: Cambridge, MA, USA, 2018.
98. Liu, X.; Hu, M.; Wang, M.; Song, Y.; Zhou, N.; He, L.; Zhang, Z. Novel nanoarchitecture of Co-MOF-on-TPN-COF hybrid: Ultralowly sensitive bioplatform of electrochemical aptasensor toward ampicillin. *Biosens. Bioelectron.* **2019**, *123*, 59–68. [CrossRef]
99. Liu, C.-S.; Sun, C.-X.; Tian, J.-Y.; Wang, Z.-W.; Ji, H.-F.; Song, Y.-P.; Zhang, S.; Zhang, Z.-H.; He, L.-H.; Du, M. Highly stable aluminum-based metal-organic frameworks as biosensing platforms for assessment of food safety. *Biosens. Bioelectron.* **2017**, *91*, 804–810. [CrossRef] [PubMed]
100. Song, Y.; Xu, M.; Li, Z.; He, L.; Hu, M.; He, L.; Zhang, Z.; Du, M. A bimetallic CoNi-based metal− organic framework as efficient platform for label-free impedimetric sensing toward hazardous substances. *Sens. Actuators B Chem.* **2020**, *311*, 127927. [CrossRef]
101. Zhou, N.; Ma, Y.; Hu, B.; He, L.; Wang, S.; Zhang, Z.; Lu, S. Construction of Ce-MOF@ COF hybrid nanostructure: Label-free aptasensor for the ultrasensitive detection of oxytetracycline residues in aqueous solution environments. *Biosens. Bioelectron.* **2019**, *127*, 92–100. [CrossRef]
102. He, H.; Wang, S.-Q.; Han, Z.-Y.; Tian, X.-H.; Zhang, W.-W.; Li, C.-P.; Du, M. Construction of electrochemical aptasensors with Ag (I) metal− organic frameworks toward high-efficient detection of ultra-trace penicillin. *Appl. Surf. Sci.* **2020**, *531*, 147342. [CrossRef]
103. Song, Y.; Xu, M.; Liu, X.; Li, Z.; Wang, C.; Jia, Q.; Zhang, Z.; Du, M. A label-free enrofloxacin electrochemical aptasensor constructed by a semiconducting CoNi-based metal–organic framework (MOF). *Electrochim. Acta* **2021**, *368*, 137609. [CrossRef]
104. Meng, X.; Gu, H.; Yi, H.; He, Y.; Chen, Y.; Sun, W. Sensitive detection of streptomycin in milk using a hybrid signal enhancement strategy of MOF-based bio-bar code and target recycling. *Anal. Chim. Acta* **2020**, *1125*, 1–7. [CrossRef]
105. Yin, C.; Zhuang, Q.; Xiao, Q.; Wang, Y.; Xie, J. Electropolymerization of poly (methylene blue) on flower-like nickel-based MOFs used for ratiometric electrochemical sensing of total polyphenolic content in chrysanthemum tea. *Anal. Methods* **2021**, *13*, 1154–1163. [CrossRef] [PubMed]
106. Liu, H.; Hassan, M.; Bo, X.; Guo, L. Fumarate-based metal-organic framework/mesoporous carbon as a novel electrochemical sensor for the detection of gallic acid and luteolin. *J. Electroanal. Chem.* **2019**, *849*, 113378. [CrossRef]
107. Yan, Y.; Bo, X.; Guo, L. MOF-818 metal-organic framework-reduced graphene oxide/multiwalled carbon nanotubes composite for electrochemical sensitive detection of phenolic acids. *Talanta* **2020**, *218*, 121123. [CrossRef]
108. Ling, W.; Liew, G.; Li, Y.; Hao, Y.; Pan, H.; Wang, H.; Ning, B.; Xu, H.; Huang, X. Materials and techniques for implantable nutrient sensing using flexible sensors integrated with metal–organic frameworks. *Adv. Mater.* **2018**, *30*, 1800917. [CrossRef]
109. Venkadesh, A.; Mathiyarasu, J.; Radhakrishnan, S. Voltammetric Sensing of Caffeine in Food Sample Using Cu-MOF and Graphene. *Electroanalysis* **2021**, *33*, 1007–1013. [CrossRef]
110. Raj, C.R.; Tokuda, K.; Ohsaka, T. Electroanalytical applications of cationic self-assembled monolayers: Square-wave voltammetric determination of dopamine and ascorbate. *Bioelectrochemistry* **2001**, *53*, 183–191. [CrossRef]
111. Gayathri, P.; Ramanujam, K. Redox active cobalt-bipyridine metal organic framework-nafion coated carbon nanotubes for sensing ascorbic acid. *J. Electrochem. Soc.* **2018**, *165*, B603. [CrossRef]
112. Li, Q.; Zheng, S.; Hu, X.; Shao, Z.; Zheng, M.; Pang, H. Ultrathin Nanosheet Ni-Metal Organic Framework Assemblies for High-Efficiency Ascorbic Acid Electrocatalysis. *ChemElectroChem* **2018**, *5*, 3859–3865. [CrossRef]
113. Valizadeh, H.; Tashkhourian, J.; Abbaspour, A. A carbon paste electrode modified with a metal-organic framework of type MIL-101 (Fe) for voltammetric determination of citric acid. *Microchim. Acta* **2019**, *186*, 455. [CrossRef]
114. Freire, C.; Fernandes, D.M.; Nunes, M.; Abdelkader, V.K. POM & MOF-based Electrocatalysts for Energy-related Reactions. *ChemCatChem* **2018**, *10*, 1703–1730.
115. Wang, X.-L.; Song, G.; Lin, H.-Y.; Wang, X.; Liu, G.-C.; Rong, X. Polyoxometalate-induced different metal–organic frameworks based on isonicotinic acid and AgI ion: Syntheses, structures and properties. *Inorg. Chem. Commun.* **2017**, *84*, 168–173. [CrossRef]
116. Fernandes, D.M.; Barbosa, A.D.; Pires, J.; Balula, S.S.; Cunha-Silva, L.; Freire, C. Novel composite material polyoxovanadate@ MIL-101 (Cr): A highly efficient electrocatalyst for ascorbic acid oxidation. *ACS Appl. Mater. Interfaces* **2013**, *5*, 13382–13390. [CrossRef] [PubMed]
117. Wang, Q.; Gu, C.; Fu, Y.; Liu, L.; Xie, Y. Ultrasensitive electrochemical sensor for luteolin based on zirconium metal-organic framework UiO-66/reduced graphene oxide composite modified glass carbon electrode. *Molecules* **2020**, *25*, 4557. [CrossRef] [PubMed]
118. Gao, F.; Tu, X.; Ma, X.; Xie, Y.; Zou, J.; Huang, X.; Qu, F.; Yu, Y.; Lu, L. NiO@ Ni-MOF nanoarrays modified Ti mesh as ultrasensitive electrochemical sensing platform for luteolin detection. *Talanta* **2020**, *215*, 120891. [CrossRef] [PubMed]
119. Xie, J.; Cheng, D.; Li, P.; Xu, Z.; Zhu, X.; Zhang, Y.; Li, H.; Liu, X.; Liu, M.; Yao, S. Au/metal–organic framework nanocapsules for electrochemical determination of glutathione. *ACS Appl. Nano Mater.* **2021**, *4*, 4853–4862. [CrossRef]